



Institute of Electrical Engineering

Slovak Academy of Sciences

841 04 Bratislava, Dúbravská cesta 9, Slovak Republic

Final Report, October 2005

Transverse resistivity of YBCO coated conductors for AC use

Award No: FA8655-03-1-3082, Effective date: 1. November 2004

Option 1, Item 1002

Bratislava, October 2005

REPORT DOCUMENTATION PAGE				41Form Approved OMB No. 0704-0188	
<p>Public reporting burden for this collection of information is estimated to average 1 hour per response, including the time for reviewing instructions, searching existing data sources, gathering and maintaining the data needed, and completing and reviewing the collection of information. Send comments regarding this burden estimate or any other aspect of this collection of information, including suggestions for reducing the burden, to Department of Defense, Washington Headquarters Services, Directorate for Information Operations and Reports (0704-0188), 1215 Jefferson Davis Highway, Suite 1204, Arlington, VA 22202-4302. Respondents should be aware that notwithstanding any other provision of law, no person shall be subject to any penalty for failing to comply with a collection of information if it does not display a currently valid OMB control number.</p> <p>PLEASE DO NOT RETURN YOUR FORM TO THE ABOVE ADDRESS.</p>					
1. REPORT DATE (DD-MM-YYYY)		2. REPORT TYPE Final Report		3. DATES COVERED (From – To) 1 November 2003 - 01-Nov-05	
4. TITLE AND SUBTITLE Transverse Resistivity of YBCO Coated Conductors for AC Use.			5a. CONTRACT NUMBER FA8655-03-1-3082		
			5b. GRANT NUMBER		
			5c. PROGRAM ELEMENT NUMBER		
6. AUTHOR(S) Dr. Milan Polak			5d. PROJECT NUMBER		
			5d. TASK NUMBER		
			5e. WORK UNIT NUMBER		
7. PERFORMING ORGANIZATION NAME(S) AND ADDRESS(ES) Institute of Electrical Engineering Dubravska 9 Bratislava 84104 Slovak Republic				8. PERFORMING ORGANIZATION REPORT NUMBER N/A	
9. SPONSORING/MONITORING AGENCY NAME(S) AND ADDRESS(ES) EOARD PSC 802 BOX 14 FPO 09499-0014				10. SPONSOR/MONITOR'S ACRONYM(S)	
				11. SPONSOR/MONITOR'S REPORT NUMBER(S) SPC 03-3082	
12. DISTRIBUTION/AVAILABILITY STATEMENT Approved for public release; distribution is unlimited.					
13. SUPPLEMENTARY NOTES					
14. ABSTRACT This report results from a contract tasking Institute of Electrical Engineering as follows: The Grantee will identify and understand factors affecting the transverse resistivity of filamentary YBCO coated conductors and to study methods to control them. The boundary resistivities of the boundaries between the substrate material (Ni or Ni-alloys) and YBCO, as well as between YBCO and the metal layer deposited to stabilize the conductor electromagnetically will be determined. Additional metal layers deposited on the thin layer of Ag or Au protecting the conductor surface will be prepared and studied. The effect of an inhomogeneity on the electromagnetic properties of the coated YBCO tapes will be investigated. In collaboration with USAF laboratory in Dayton striated tapes prepared using laser technique instead of photolithography will be investigated. Finally, a model AC conductor will be designed.					
15. SUBJECT TERMS EOARD, Aircraft Subsystem, Power, Superconductivity					
16. SECURITY CLASSIFICATION OF:			17. LIMITATION OF ABSTRACT UL	18, NUMBER OF PAGES 41	19a. NAME OF RESPONSIBLE PERSON MICHAEL KJ MILLIGAN, Lt Col, USAF
a. REPORT UNCLAS	b. ABSTRACT UNCLAS	c. THIS PAGE UNCLAS			19b. TELEPHONE NUMBER (Include area code) +44 (0)20 7514 4955

This work was performed at the Department of electrodynamics of superconductors, Institute of Electrical Engineering, by:

E. Demencik
D. Erbenova
L. Jansak
J. Kvitkovic
P. Mozola
M. Polak (principal investigator)
J. Ryza
J. Talapa
E. Usak
P. Usak

Content

1. Introduction and goals.....	4
2. Studies on short samples of YBCO coated conductors.....	5
2.1. External field AC losses in YBCO samples “B”	5
2.2. Current distribution in YBCO tapes	5
3. Electromagnetic properties of test YBCO coils.....	11
3.1. AC losses in YBCO coils and a comparison with the properties of a copper coil. 11	
3.2. Effects of winding magnetization on the magnetic field produced by the pancake coil YBCO 13_2m wound with YBCO coated conductor (II.G).....	13
Conclusions	24
APPENDIX A	26
APPENDIX B	31
APPENDIX C	37

1. Introduction and goals

The application of superconductors could improve the properties of electrical devices by a substantial way. The lightweight aircraft power generator is one of possible applications of the second generation of high temperature coated conductors YBCO (II G).

The successful realization of a superconducting winding with the required properties needs a high current and low loss AC HTS conductor with properties described in details in the paper of Oberly et al. [1].

Our preceding projects were concentrated on some problems of the development and properties of a suitable YBCO based conductor. This work is focused on problems related to the current distribution in YBCO striated (filamentary) samples and on YBCO coils. The main goal is to investigate and evaluate parameters of YBCO coils operating with DC and AC currents.

One of important results of the research, focused on the development of AC YBCO conductors, is the reduction of the hysteresis losses. The reduction was successfully achieved by subdividing the continuous YBCO layer into narrow filaments. However, the technology of the striation (filamentation) of the continuous YBCO layer may produce electrical contacts between the filaments and the metallic substrate. As a result, the filaments become coupled and additional losses (coupling losses) are produced. The reduction of these losses needs so called filament transposition, which is a very difficult problem. One of the possible solutions is the use of the saddle type windings, where the transposition is realized by an appropriate bending of the striated tape.

The separation of the coupling losses from the total losses of a sample was one important issue of our work. We will present the loss measurements in wide interval of frequencies and explain the procedure of the determination of the transverse resistivities, which allow to compare the coupling losses in the measured samples.

The current distribution in a filamentary YBCO tape influences its behavior by a substantial way. As mentioned in [2], an interruption of 1 filament can bloc the current flow in it and reduce the current carrying capacity of the tape. A possible solution of this problem is the concept of multiply connected filaments proposed in [2]. To be able to determine the current distribution in these tapes and to understand the measurement results we performed a series of measurements in filaments supplied individually. We also studied magnetic field in the vicinity of samples carrying transport or magnetization currents. The properties of the bridges between the neighboring filaments can affect the behavior of the samples. Thus, we also studied their properties.

In general, the extension of short sample experiments (critical current, AC losses) on coils with tape length much longer than the short sample length, is not a simple task. Because of that we think that the experiments on coils can provide very useful information for the development of new types of AC conductors. As a first step, we

studied the DC and AC behavior of test coils wound with non-striated YBCO coated conductor. In the frame of this work we received 3 small YBCO coils, previously used in the high field DC measurements, from our partners in WPAFB. The coils were manufactured by American Superconductors. We studied the DC critical current of the coils, the radial field component at the edges of the coils as well as the consequences of large magnetization currents on the magnetic field vs. coil current characteristics. The main effort was given to the determination of AC losses in the wide range of frequencies from 60 Hz to 1000 Hz.

2. Studies on short samples of YBCO coated conductors

2.1. External field AC losses in YBCO samples “B”

The main goal of this study was to elaborate a procedure for determination of the coupling losses from the measurements of the total losses.

We proposed and tested a two steps procedure. In the first step we measured the frequency dependence of the total losses at low frequencies at a constant field amplitude in the interval from about 1 mHz to 100 mHz. At these low frequencies the coupling losses are negligible and the hysteresis losses, W_{hyst} , prevail. From the dependence $W_{\text{hyst}} = f(f)$ we determine the dependence dW_{hyst}/df , which is of the order of $\sim 10\%$ of W_{hyst} .

The results are summarized in a paper presented at the international conference EUCAS 2005 in Vienna, see **APPENDIX A**.

2.2. Current distribution in YBCO tapes

To reduce the hysteresis losses in YBCO coated conductors, the YBCO layer must be subdivided into narrow filaments separated by small gaps. The uniformity of the current distribution in the filaments is the basic requirement for the successful function of the filamentary tape.

The previous experiments on AC losses in samples B/1, B/2, B/3, B/4 and B/5 showed that in some areas of the filamentary tapes the filaments have an electrical contact with the metallic substrate.

Here we describe our experiments focused on the understanding of the current distribution. The main goal is to elaborate a suitable method for measurement of the current distribution.

The goals of the experiments:

- a. To determine the critical currents of each filament supplied separately
- b. To determine I-V curve of the filamentary tape with potential taps attached to different filaments
- c. To determine the current distribution in the filamentary tape

Experimental:

A special sample holder was designed as shown in Fig 2.2.1. Each filament was connected with the current lead by a thin copper wire. This system allowed to pass the current through 1 filament separately and to disconnect all other filaments. The detail showing the connections of filaments with copper wires see Fig 2.2.2.

Sample holder were designed for the samples 10 x 100 mm.

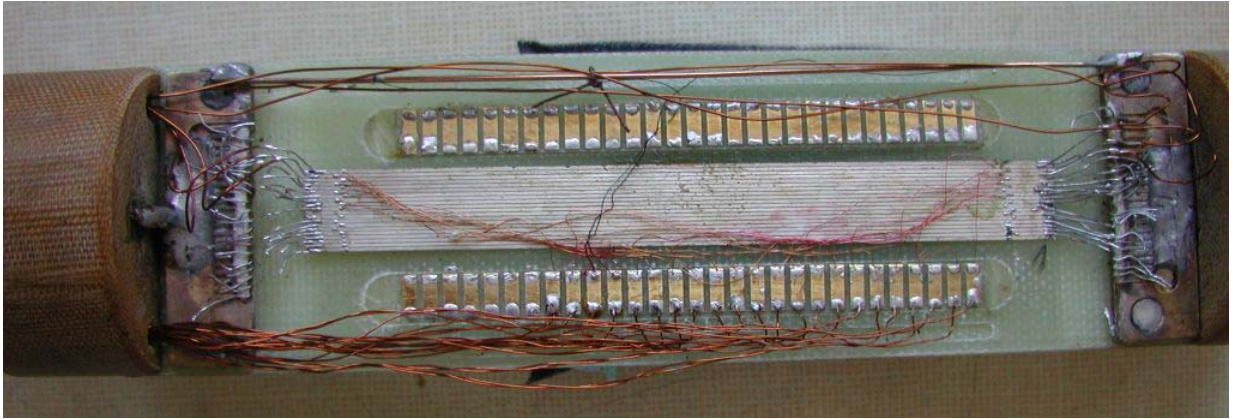


Fig.2.2.1 The sample holder with filamentary sample. All filaments are supplied via a thin copper wire

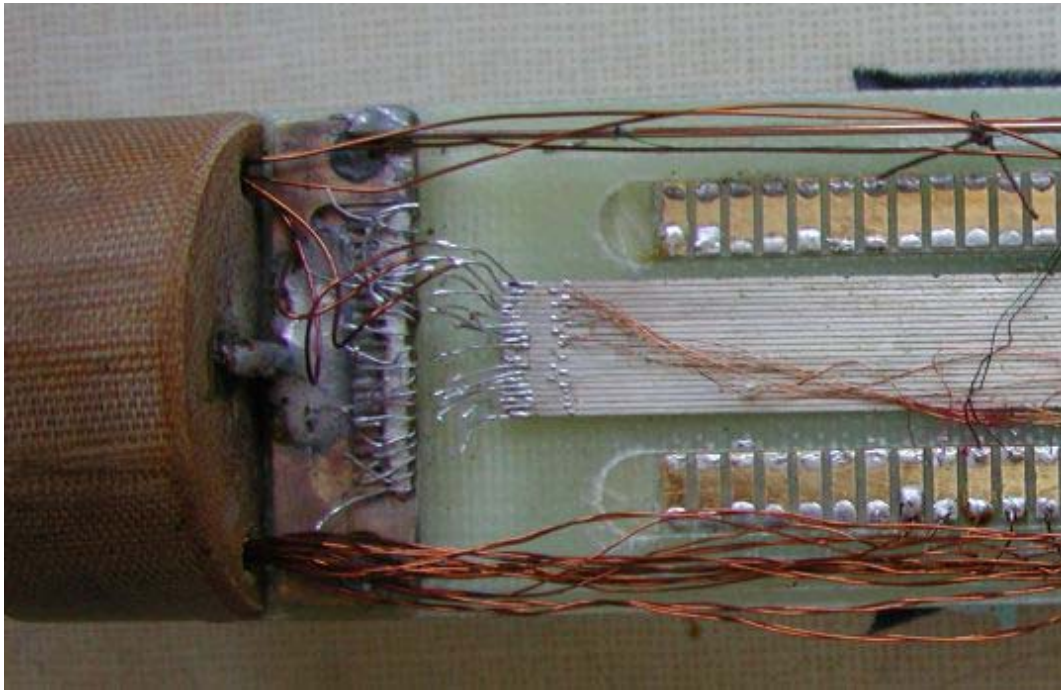


Fig.2.2.2. The connections between the filaments and the current lead and the potential taps

Results of experiments:

Sample B/4

The sample has 20 filaments 0.5 mm wide, the filaments extend over the whole tape length.

Experiment 1: Measurement of the field profile in the vicinity of the filamentary sample B/4 at 300 K. Only 1 filament (filament “10”) was supplied by the current at room temperature $T = 300$ K. The results of the measurements $B_z = f(x)$ at various distances “ z ” and the calculated values are shown in the next Figures 2.2.3a and 2.2.3b:

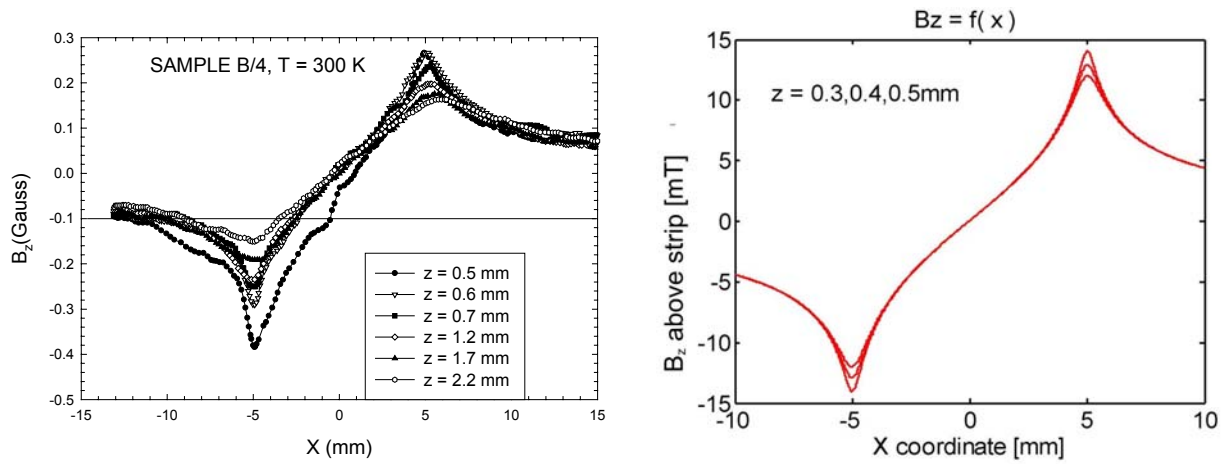


Fig.2.2.3: **a**-Measurements: $B_z = f(x)$ at various distances “ z ” for sample B/4, only one filament (filament 10) supplied, $I_f = 0.47$ A ; **b**- The calculated values of B_z vs x assuming the homogeneous current distribution

Conclusion: The measured field profile at 300 K clearly shows that the current flows in the whole tape width when only 1 filament is supplied. Thus, the filaments are electrically interconnected by the substrate.

Experiment 2: Measurement of the field profile in the vicinity of the filamentary sample B/4 at 77 K, only 1 filament is supplied by the current

Only 1 filament (filament “10”) was supplied, the sample was immersed in liquid nitrogen, $T = 77$ K. We measured $B_z = f(x)$ at the distance “ z ” = 0.3 mm, the results are shown in Fig. 2.2.4a. The calculations of $B_z = f(x)$ for 1 filament supplied are shown in Fig. 2.2.4.b

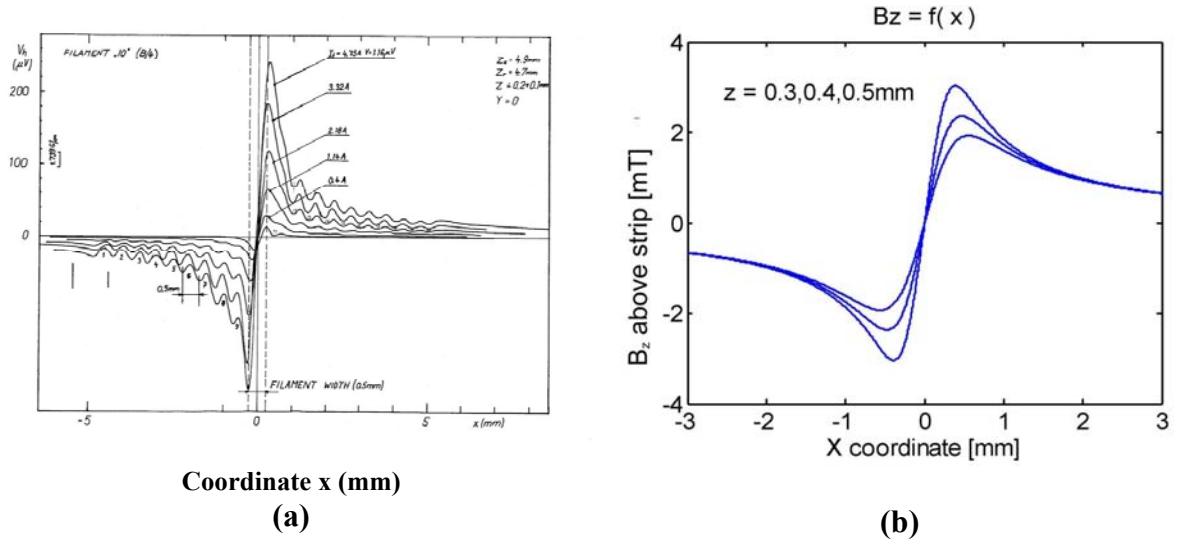


Fig. 2.2.4: a- The measured curves $B_z = f(I)$ at 77 K, only filament 10 supplied; b - The calculated curve $B_z = f(x)$

The shape $B_z = f(x)$ clearly shows that the current I_f flows in one filament (filament “10”). Magnetic field produced by the current I_f (in filament “10”) induces magnetization currents in the neighboring filaments, which produce again magnetic field superimposed on the field created by I_f .

This experiment show that the short-circuits filaments-substrate-filament are not superconducting!

Sample P3

Sample P3 is a YBCO sample 10 cm long, 12 mm wide. It is divided into 24 stripes (one stripe at the edge is about 1.5 x wider than the rest). The length of the striated part is 7 cm. There are non striated margins 1.5 cm on both ends. The critical current before striation was 160 A.

Penetration of the magnetic field into sample P3

With this sample we measured the external field penetration into the sample with the aim to determine the uniformity of the current distribution between the filaments.

In Fig. 2.2.5 we show the field measured 0.6 mm above the sample surface at various values of the external magnetic field. The field was increased stepwise from zero to 58.8 mT.

SAMPLE YBCO AFOSR P3 T=77 K, B_UP.JNB

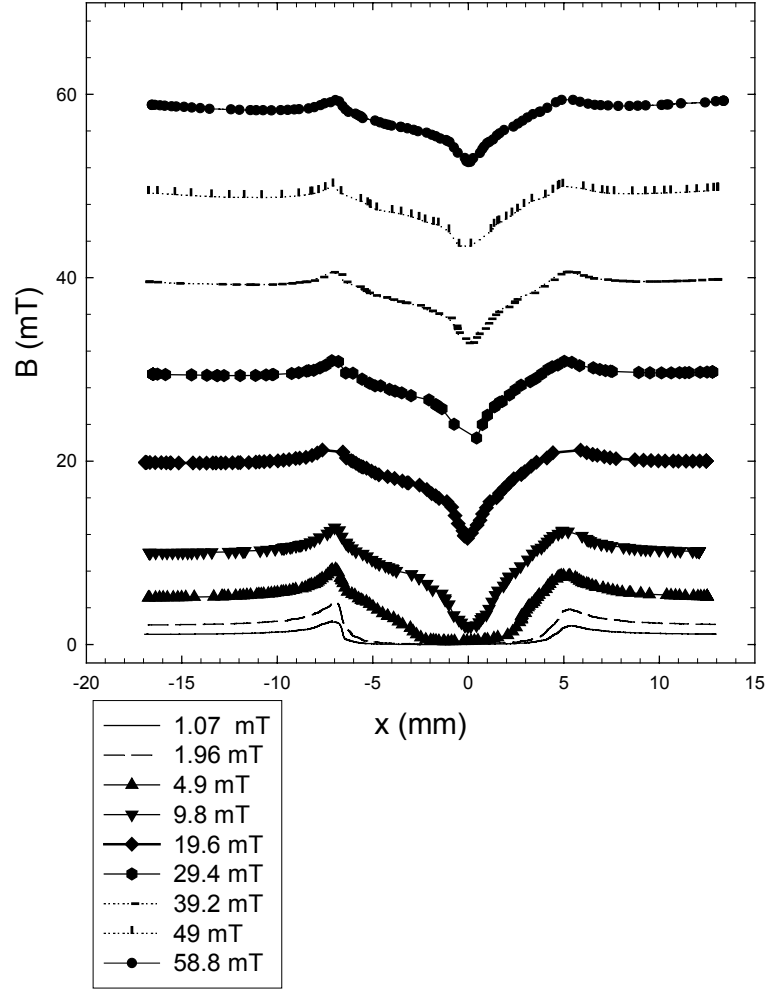


Fig.2.2.5: The magnetic field B_z measured in the distance of 0.6 mm above sample P3 at the external magnetic field increasing stepwise from 0 up to 58.8 mT

In the Figure 2.2.5. we see that at fields 1.07 mT and 1.96 mT the field penetrated into the sample at the edges only. At 9.8 mT the sample is already penetrated. At higher field the field profile indicates that the current distribution across the sample is not uniform.

It is also evident that the magnetization currents create loops which close at the sample ends via the non-striated sections of the tape. So, the filaments are not seen in the profiles B_z vs. x .

After this experiment we supplied the sample by a transport current and measured the corresponding field profile. However, at $I = 0$ we measured the field due to the persistent currents induced during the previous experiment. The results are shown in Fig.2.2.6.

SAMPLE YBCO AFOSR P3,
increasing transport current

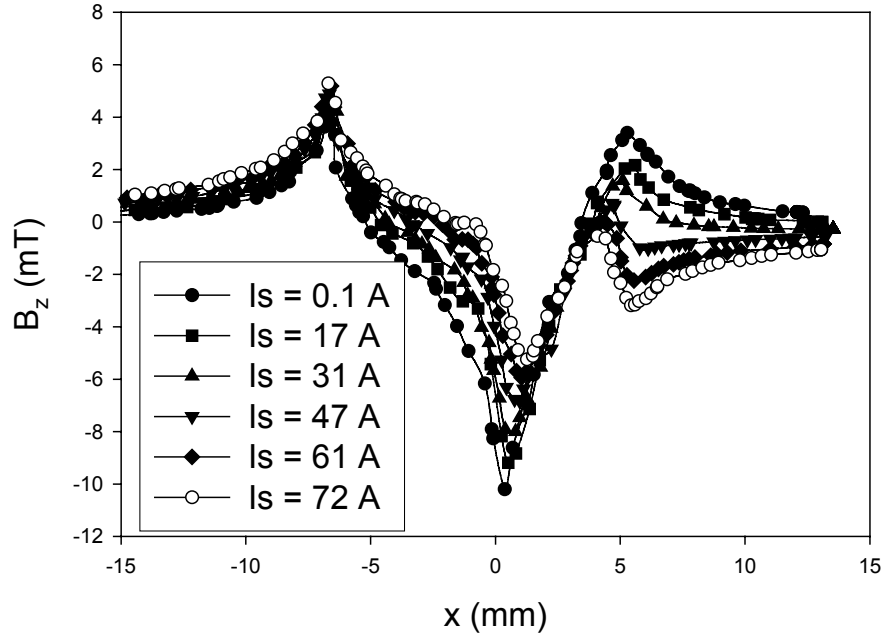


Fig. 2.2.6. The measured profiles $B_z = f(I)$ measured at various values of the transport current, which was increased stepwise.

At current $I \sim 80$ A the current abruptly decreased to zero due to burning of the sample close to one of the current contacts. The photograph of the damaged sample is shown in Fig.2.2.7. We do not know the reasons of the damage at the moment. As mentioned, the sample before the striation had the critical current of 160 A. Further experiments aimed to find the reasons of the sample damaged are planned.



Fig.2.2.7: The damaged sample P3 (unfortunately, the microphotograph is not clear enough)

The magnetic field in the vicinity of the samples can be used to determine the current distribution across the sample by solving the inverse problem. We developed a procedure and calculated the distribution of the current across the tape carrying magnetization or transport currents. The description of the results is given in **APPENDIX B**.

3. Electromagnetic properties of test YBCO coils

3.1. AC losses in YBCO coils and a comparison with the properties of a copper coil

We received 3 YBCO coils, manufactured by American Superconductors, which were previously tested in high magnetic fields:
YBCO N° 6, YBCO N°10 and YBCO N°12.

The main coil data provided by American Superconductors are:

Coil number	Conductor length (m)	turns	$I_c(A)$	n
#6	1.2	10	132	29
#10	0.4	4-5	177	37
13	1.2	158	158	~30

The measurement of AC losses showed that for all 3 coils they are much larger than expected. The measured AC losses in coils “as received” with 500 Hz and $I_{\text{rms}} = 50$ A are:

Coil #6	7.0 W
Coil#10	2.1 W
Coil#12	17.0 W

The following investigations revealed that there were short-circuited copper tape turns in the coils. The copper tapes pieces were attached to the current leads to improve the cooling.

A photograph of the disassembled current contact illustrating the situation is shown in Fig.3.1.1.

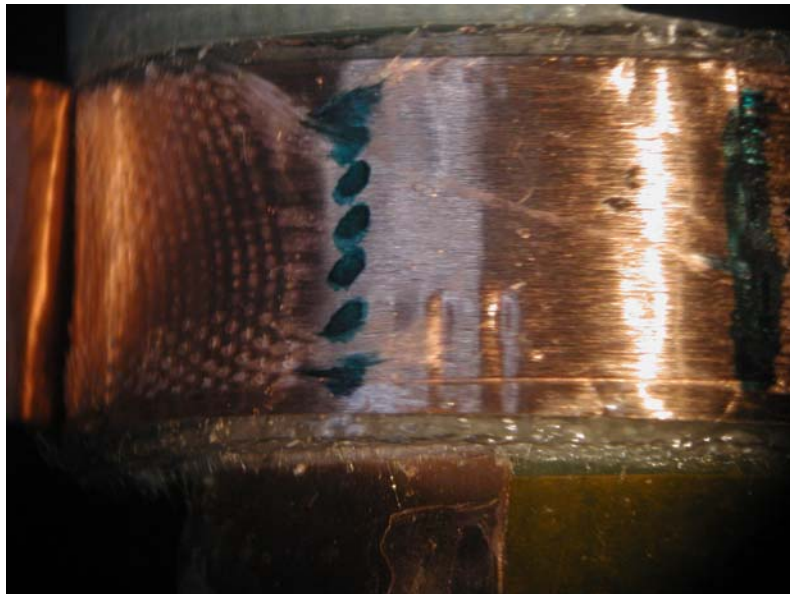


Fig.3.1.1: A photograph of the disassembled outer contact showing the insufficient length of the insulation

As a result, the AC losses at 50 A_{rms} and 500 Hz were reduced from 17 to ~ 4 W.

We carefully removed the short circuits in the coil 13. The coil was renamed to YBCO 13_2m and measured. The results and analysis are described in the contribution to the international conference Magnet Technology 2005 held in Genova, Italy, September 2005.

The full text of the contribution is in **APPENDIX C**.

3.2. Effects of winding magnetization on the magnetic field produced by the pancake coil YBCO 13_2m wound with YBCO coated conductor (II.G)

The magnetic fields created by DC current flowing in superconducting coils are usually calculated by the same way as those created by resistive coil [3], which is shown in Fig. 3.2.1.

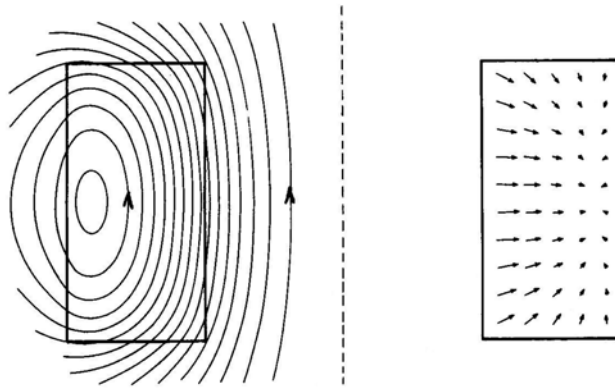


Fig. 3.2.1: The lines of the magnetic flux produced by a pancake coil wound with a normal with uniform current distribution.

The aim of this study is to identify and understand the differences in the behavior of a coil wound with YBCO tape (II.G) from a similar coil with a normal conductor (copper).

The basic difference is the different current density distribution: uniform distribution in the resistive coil and non-uniform distribution in the coil wound with a superconducting tape.

Brandt and Indenbom [4] calculated the distribution of the transport current in a thin, wide superconducting tape and the distribution of the magnetization currents of the tape exposed to a homogeneous external magnetic field. They showed that the current penetrates into the tape from the edges, so that the current distribution across the tape width is non very uniform at $I \ll I_c$. We observed this behavior in experiments with the short sample P3. However, in the pancake coil the magnetic field is highly non-uniform. The perpendicular components of the magnetic field at the coil edges induce magnetization currents which considerably affect the magnetic field inside and outside the winding. Moreover, the magnetization currents give rise to hysteresis effects. As a results, the behavior of a pancake coil wound with YBCO tape could be very different from that of the similar resistive coil.

We studied magnetic fields outside the winding of the experimental YBCO coil YBCO 13_2m. Special Hall probes with the small active area were used to measure the magnetic field. Hall Probe HP 1 (No.40) measures the longitudinal field component B_z along the coil axis, Hall Probe HP 2 measures the axial field component, B_z , at the constant distance $r = 12$ mm from the coil axis in dependence on the axial position z and Hall Probe HP 3 measures the radial field component, B_r , as a function of the position z at the constant radial position $r = 11.2$ mm (see Fig. 3.2. 2):

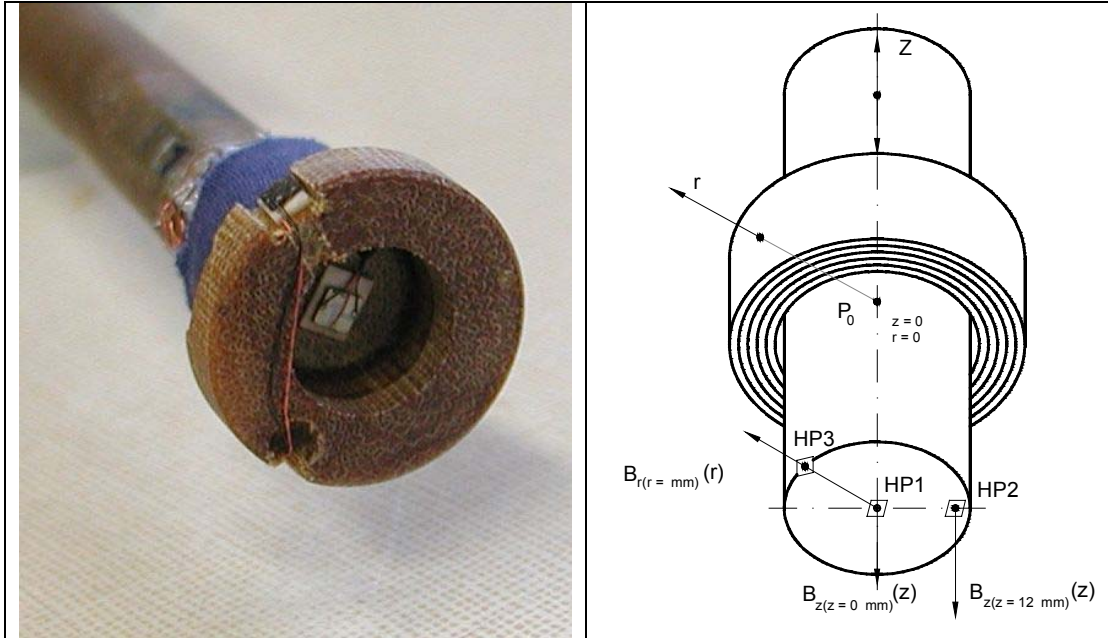


Fig.3.2.2. A sketch showing the positions of Hall probes HP1, HP2 and HP3

a. Measurements of $B_z(r = 0)$ at room and liquid nitrogen temperature at low coil currents

At first, we measured the longitudinal field along the coil axis $B_z(r = 0) = f(z)$. The radial field component in the point $z = 0$ is zero, in any other values of z the radial field component exists. At room temperature the current is uniformly distributed across the tape and flows in the copper stabilization layer only. In any point the field is directly proportional to the coil current

$$B(x,r) = k I$$

The situation is similar to that illustrated by Fig.3.2.1.

The axial field component $B_z(r = 0)$ measured along the coil axis at coil currents $I = 2$ A, 4 A and 6 A at room temperature and 77 K are shown in Fig. 3.2.3.

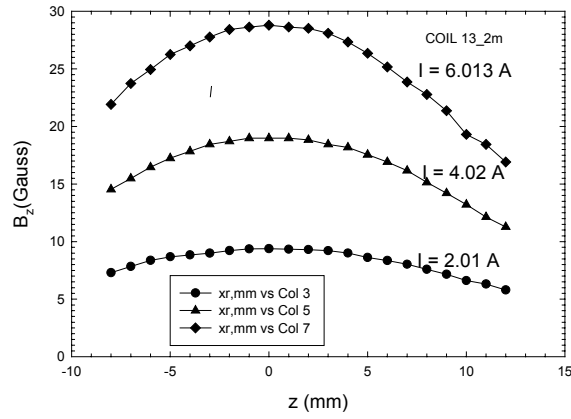


Fig.3.2.3: B_z vs. z measured at room temperature for 3 values of the current I

The field amplitude in the coil center depends linearly on the coil current. The ratio field/current at room temperature in the coil center is 4.72 G/A.

b. Measurements of $B_z(r=12 \text{ mm})$ vs. z

In this position Hall Probe is much closer to the winding and measures the longitudinal (axial) field component, B_z . The magnetic field is larger in comparison with the case $r = 0$. The profiles $B_z(r = 12 \text{ mm})$ vs. z measured at room temperature and 77 K are shown in Fig.3.2.4.

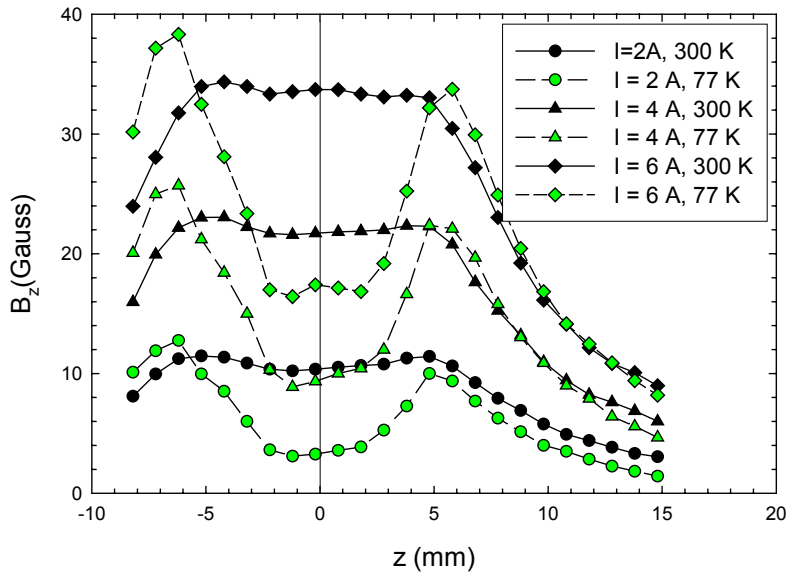


Fig.3.2.4. The field component B_z measured in the position $r = 12 \text{ mm}$ at 300 K (black symbols) and 77 K (green symbols) at various currents I (increasing branches).

As seen, the profile has a minimum at the position $z = 0$ (median plane of the coil). The maximal field component was measured at the coil ends.

c. Measurements of $B_r(r = 11 \text{ mm}) = f(z)$

The measured profiles $B_r = f(z)$ measured at room temperature and 77 K are shown in Fig. 3.2.5.

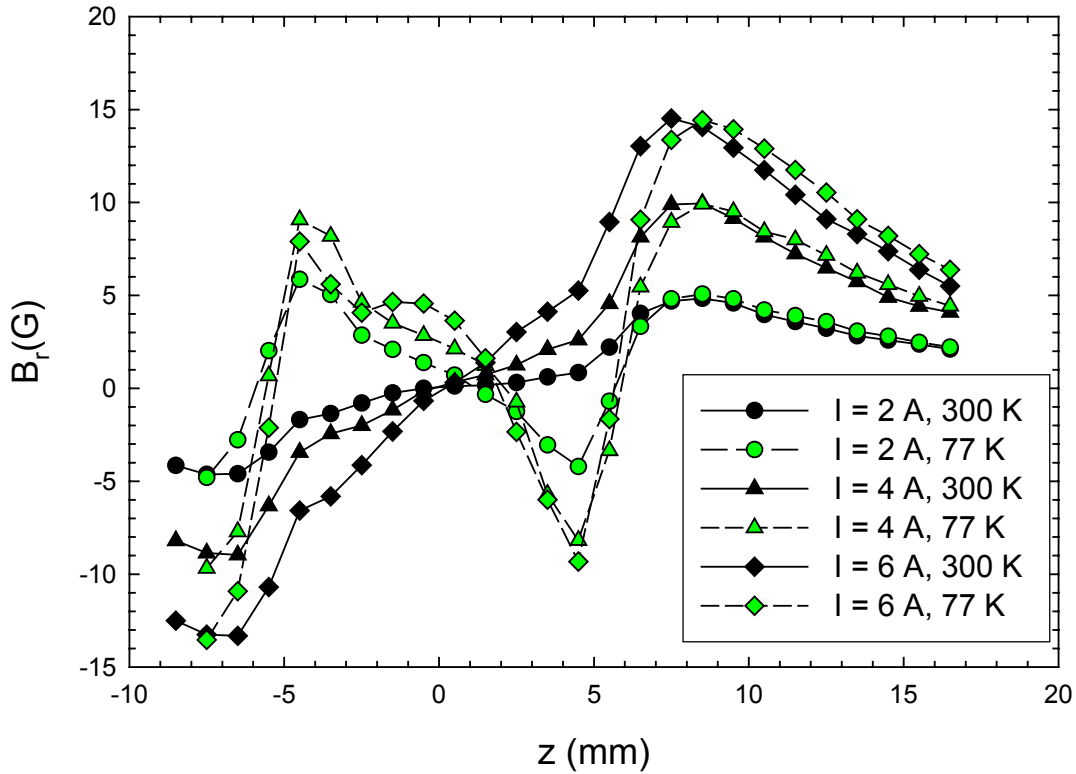


Fig.3.2.5. The radial field component, B_r , measured at 300 K and 77 K vs. z -coordinate.

In the case of the superconducting coil the field profile $B_r(z)$ is rather complicated, as seen in Fig. 3.2.5. In the coil center this component is practically zero. At the coil edges ($z = 5$ and -5 mm) there are local extremes, which have the opposite signs. Outside the coil there are 2 other extremes, which have opposite signs then those inside the coil. For larger z the values of B_r asymptotically go to zero.

The change of the sign of B_r inside the coil in comparison with the values obtained at room temperature clearly shows that this is the effect of magnetization currents. This change cannot be explained by the non-uniform distribution of the transport current only.

d. Measurements of the field components B_z and B_r during the complete cycle of the transport current $0 \rightarrow I_{\max} \rightarrow 0 \rightarrow -I_{\max} \rightarrow 0$ at low dI/dt

As mentioned, all field components should be directly proportional to the coil current in the case of the uniform distribution of the current across the tape width. This is not the case for a superconducting pancake coil wound with a tape.

First, if we increase the current, it penetrates from the edges into the tape interior, as predicted by Brandt and Indenbom. Second, the coil produces an inhomogeneous field. In each point of the winding the local current density is the critical current density corresponding to the local field [6]. The component of the coil field perpendicular to the tape $B_r(I)$ induces magnetization current, as shown in Fig.3.2.6. These currents produce a magnetic field opposite to $B_r(I)$ and reduce the perpendicular field component at the coil edges.

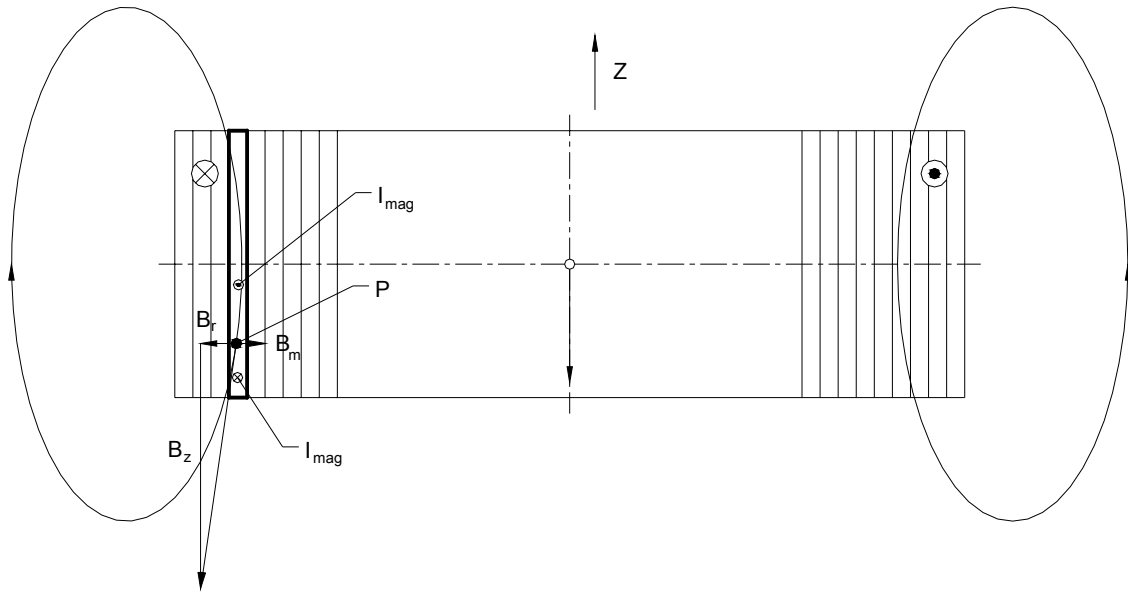


Fig.3.2.6. Sketch illustrating the induction of magnetization currents

Thus, these magnetization currents modify the coil field. As the magnetization currents depend on the sign of dI/dt , the magnetization at increasing current (dI/dt positive) is different from that at the decreasing current (dI/dt negative). Consequently,

the coil field at the same current for the increasing current are different from that for the decreasing current.

We measured the component of magnetic field produced by the coil in the positions where their amplitude is maximal:

$B_z(r=0)$ in the coil center ($z=0$): Fig. 3.2.7

$B_z(r=12\text{ mm}, z=0)$ in the median plane: Fig.3.2.8

$B_r(r=11.2\text{ mm})$ at the local maximum outside the coil ($z=+8\text{ mm}$ and -8 mm):
Fig.3.2.9

$B_z(r=12\text{ mm}, z=5\text{ mm})$ at the local maximum at the coil edge: Fig. 3.2.10.

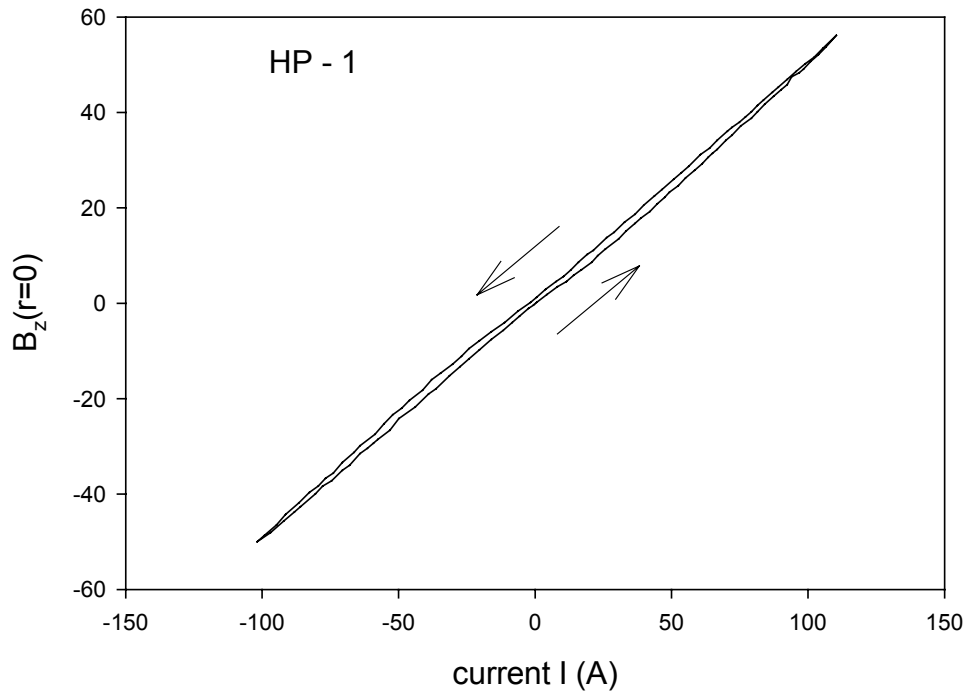


Fig.3.2.7: The axial field components vs. current for the whole cycle $0 \rightarrow I_{\max} \rightarrow 0 \rightarrow -I_{\max} \rightarrow 0$. The hysteresis is rather low due to the large distance of the measured point from the coil winding

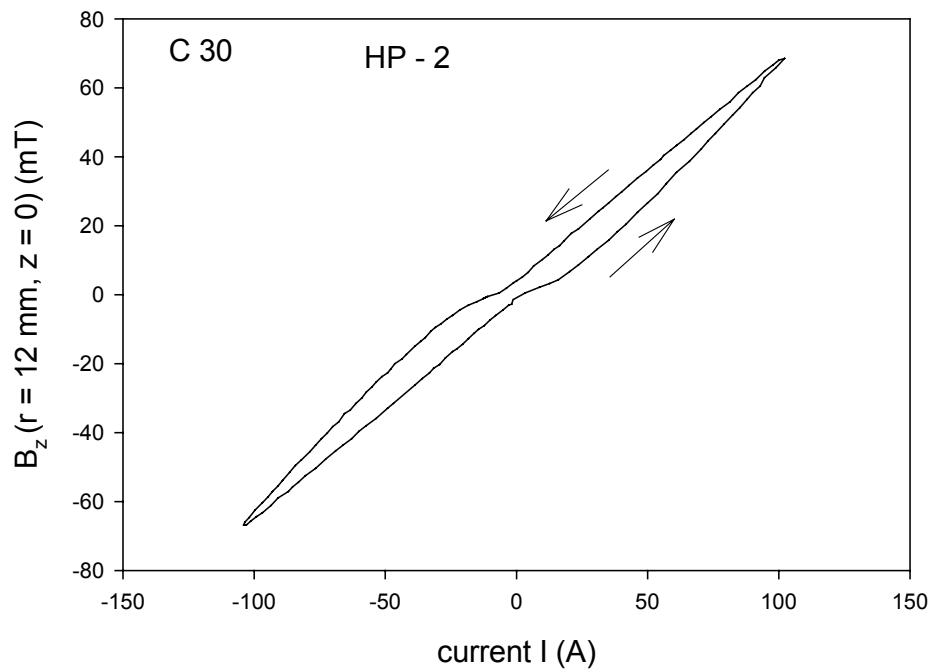


Fig. 3.2.8: The axial field component vs. coil current measured at the complete current cycle

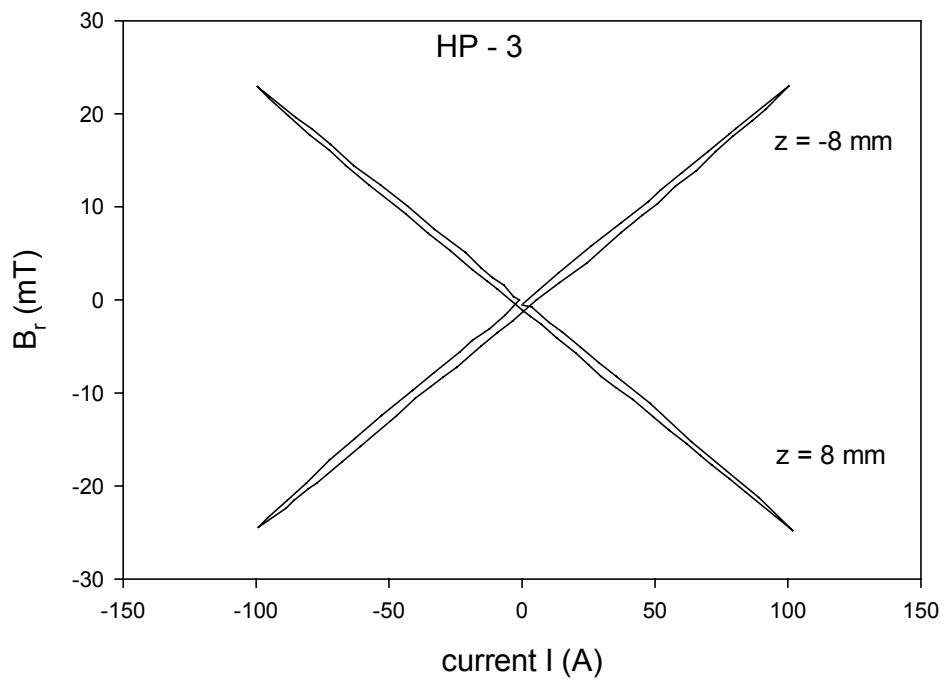


Fig. 3.2.9: The radial field component vs. current measured at the extremes outside the coil

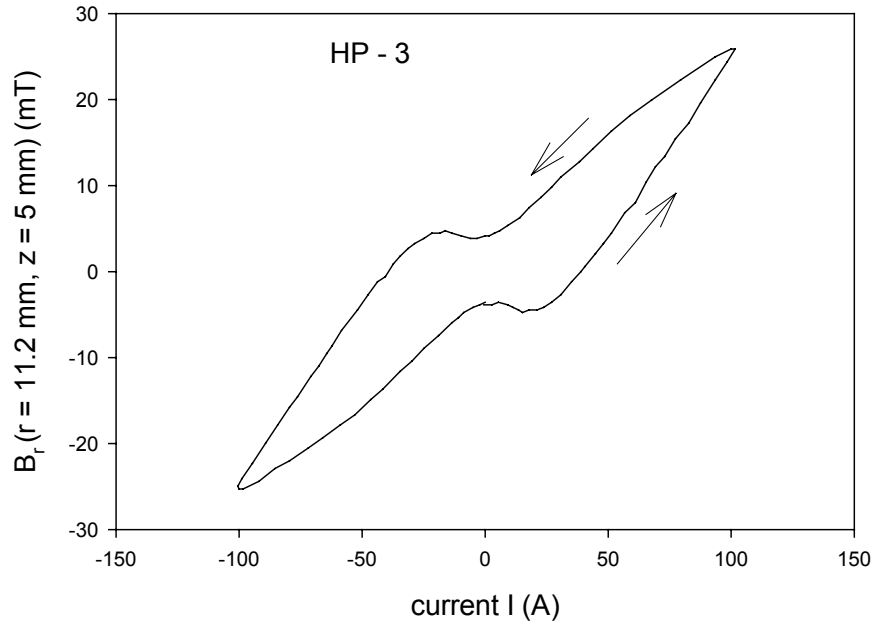


Fig.3.2.10: The radial field component at $r = 11.2$ mm measured at $z = 5$ mm (coil edge)

All measured curves have a hysteretic character. The hysteresis effects are the stronger the closer is the measured point to the winding.

e. The shape of the Hall voltage signal proportional to the radial component of the coil magnetic field, $V_h \sim B_{r,\max}$

As shown, the hysteresis effects described above affect the values of the component of the magnetic field of the coil carrying DC current. For the coil operating with AC current the magnetization currents can also modify the shape of the AC magnetic field.

In this phase of the studies we focused on the radial component, $B_{r,\max}$ measured by HP-3. We measured the Hall voltage $V_{h,\max} \sim B_{r,\max}$ at 3 frequencies: 111 Hz, 511 Hz and 911 Hz.

The measured time dependence of the Hall voltage $V_{h,\max}$ and of the coil current are shown in the following Figures 3.2.11, 3.2.12 and 3.2.13.

The Hall voltage proportional to the radial field component is not sinusoidal, which is caused by the hysteresis of the magnetic field components.

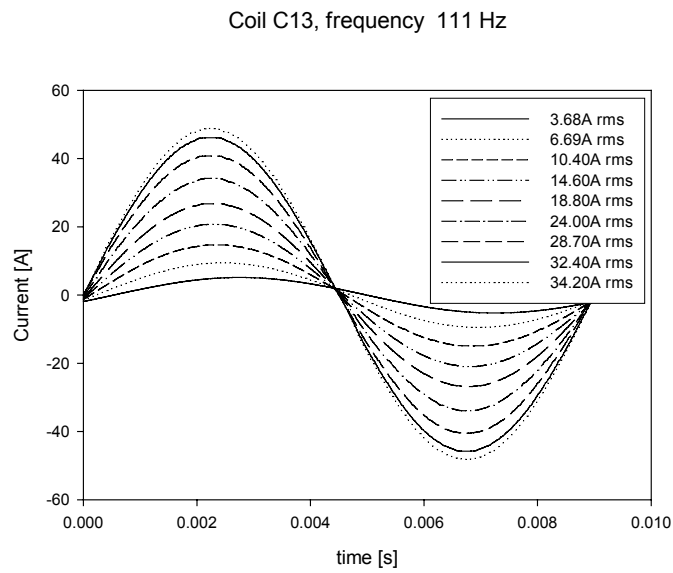
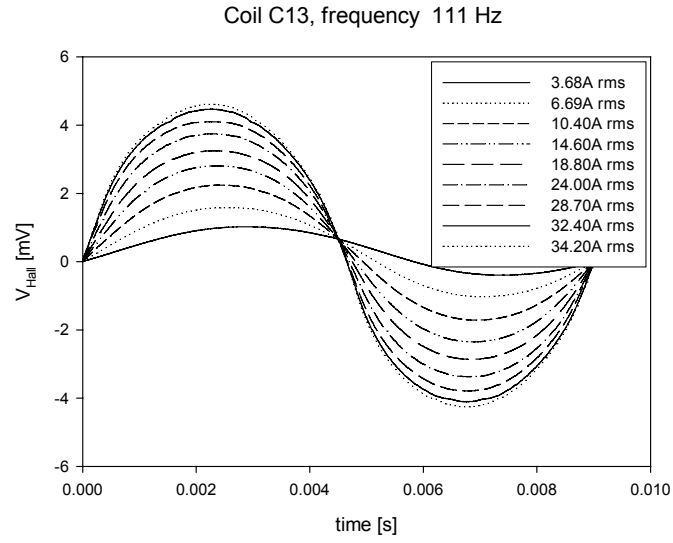


Fig.3.2.11: The time dependences of the Hall voltage and coil current at 111 Hz

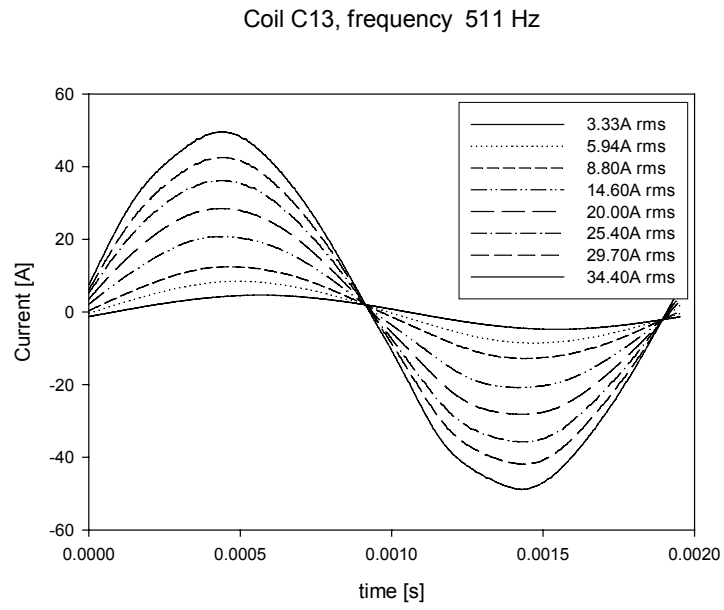
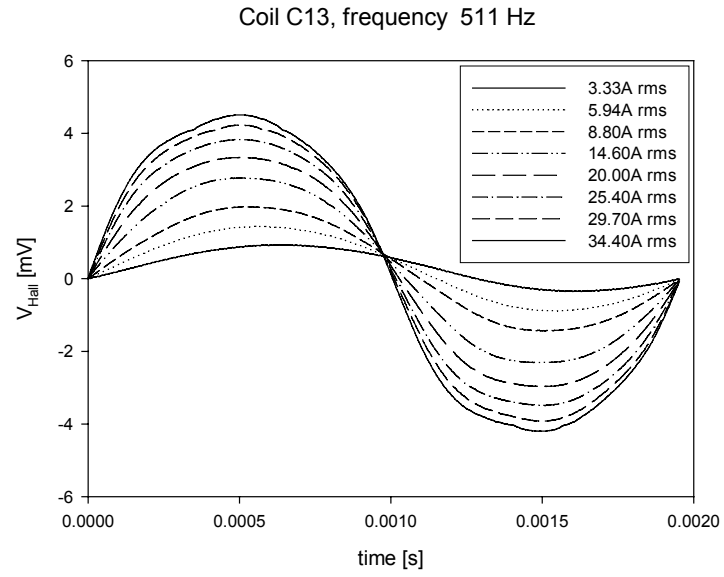


Fig.3.2.12: The time dependences of the Hall voltage and coil current at 511 Hz

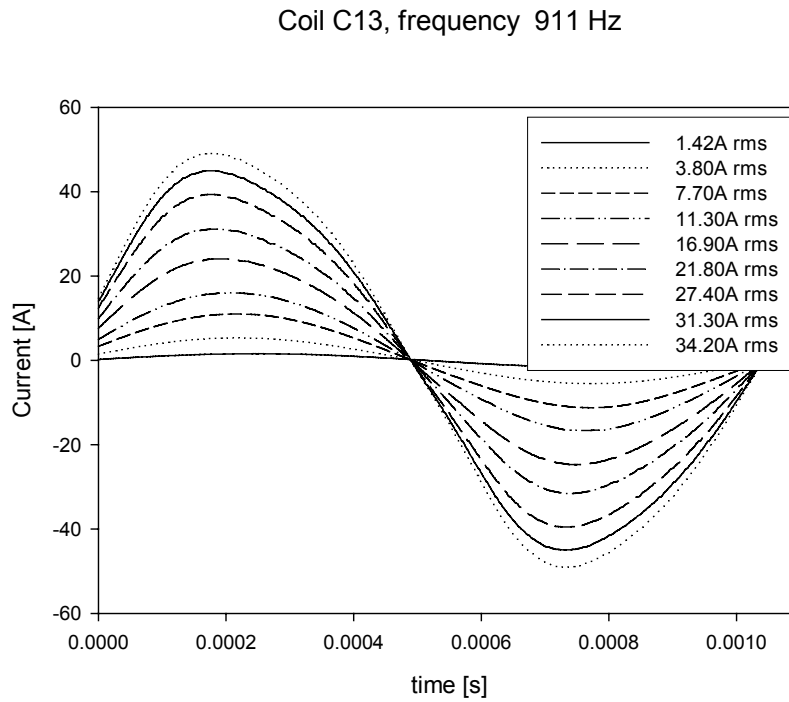
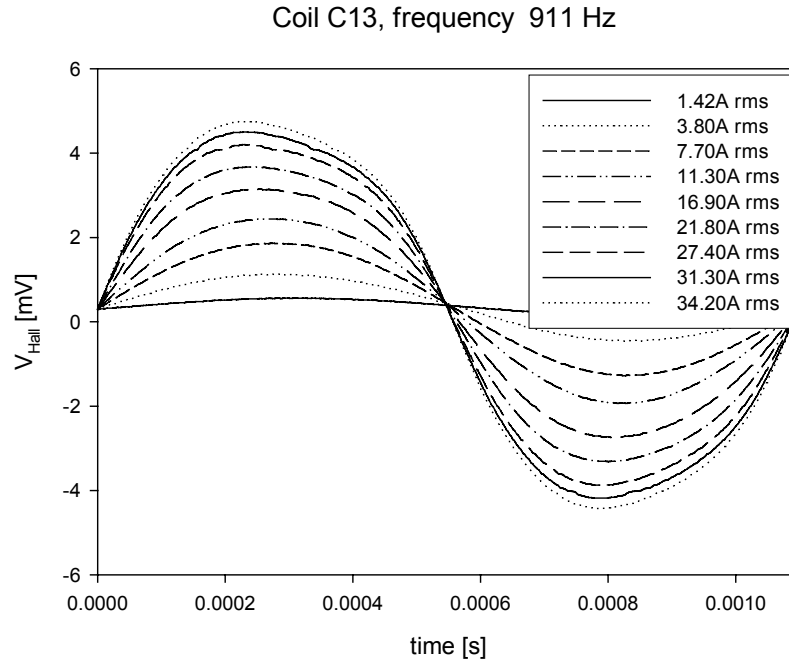


Fig.3.2.13: The time dependences of the Hall voltage and coil current at 911 Hz

Conclusions

1. We showed that in our samples of striated YBCO tapes (B/4) the YBCO filaments have good electrical contacts with the substrate. However, these contacts are not superconducting.
2. In all samples of YBCO filamentary tapes we detected coupling currents and corresponding coupling losses. We evaluated the corresponding time transverse resistivities.
3. We determined the AC losses in the model YBCO pancake coils wound with non striated YBCO tape in the frequency range from 60 Hz up to 1000 Hz and compared them with the AC losses in a similar coil made of copper tape. The YBCO coil showed lower losses in the whole frequency interval. With increasing frequency the difference in losses became smaller.
4. The component of the magnetic field created by the coil are strongly affected by the magnetization currents. The dependence of these field components on coil current is non-linear and hysteretic.
5. Due to the magnetization current the coil inductance depends on the coil current.
6. The radial field components are not sinusoidal for a sinusoidal coil current.
7. In spite of the large hysteresis losses in the non-striated tape the coil was able to operate at AC currents with frequencies up to 1000 Hz.

References:

- [1] Ch. E. Oberly, L. Long, G. L. Rhoads, W. J. Carr Jr., Cryogenics 41 (2001) 117-124
- [2] G. A. Levin, P. N. Barnes, Concept of Multiply Connected Superconducting Tapes, preprint AFRL, November 2004
- [3] R.W. Boom, R. S. Livingstone, Proceedings IRE, p.275, March 1962
- [4] E. H. Brandt, M. Indenbom, Phys. Rev. 34, pp. 12839-12906, 1993
- [5] Y. Wolfus, Y. Adanny, A. Friedman, F. Kopansky, Y. Yeshurun, EUCAS 05, Vienna 11.-15. September 2005, paper TH-P4-20

APPENDIX A

This paper was presented at the international conference EUCAS 2005, Vienna, September 12-15, 2005.

It will be published in IOP Proceedings, 2006.

Coupling losses and transverse resistivity of multifilament YBCO coated superconductors

M. Polak¹, E. Usak^{1,4}, L. Jansak¹, E. Demencik¹, G. A. Levin², P. N. Barnes², D. Wehler³, B. Moenter³

¹Institute of Electrical Engineering, Slovak Academy of Sciences, Bratislava, Slovakia, ²Wright Patterson Air Force Base, USA, ³University of Wuppertal, Germany, ⁴Slovak Technical University, Faculty of Electrical Engineering and Information Technology, Bratislava, Slovakia

The corresponding author: M. Polak, elekpola@savba.sk

Abstract. We studied the magnetization losses of four different types of filamentary YBCO coated conductors. A 10 mm wide YBCO coated conductor was subdivided into 20 filaments by laser ablation. We measured the frequency dependence of the total losses in the frequency range $0.1 \text{ Hz} < f < 608 \text{ Hz}$. The coupling loss was obtained from the total by subtracting the hysteresis loss. The latter was measured at low frequencies since only hysteresis loss is non-negligible at frequencies below 1 Hz. The transverse resistivity, ρ_{tr} , was determined from the coupling losses; it was assumed that the sample length is equal to half of the twist pitch. The values of ρ_{tr} deduced from the loss data were compared with those obtained by the four-point measurements with current flowing perpendicular to the filaments. Preliminary results indicate the existence of electrical contacts between the superconducting filaments and the substrate in some areas of the samples. This was also confirmed by the Hall probe mapping of the magnetic field in the vicinity of the tape. The measured transverse resistivity was close to the resistivity of the substrate (Hastelloy).

1. Introduction

Low loss YBCO coated conductor can enable the fully-superconducting version for motors and generators in which both the field and armature windings are superconducting [1]. To reduce hysteresis losses in tapes several millimetres wide, subdividing of the tape into narrow parallel stripes is necessary [2,3]. The resulting conductor is a multifilamentary tape with parallel thin strips (filaments) separated by narrow gaps. The striation can be done using various technologies, as the photolithography and wet etching [4] or laser micromachining [5].

The striated (filamentary) tapes become vulnerable to localized defects. This problem can be solved either by covering the filaments by sufficiently thick normal metal layer with low resistivity metal/YBCO boundary, or by making a network of superconducting bridges, which allow the current sharing between filaments [6]. As shown by Amemyia et al. [7], in filamentary tapes prepared by laser micromachining the total losses contain also a coupling loss component due to the presence of electrically conductive path between the filaments and the metallic substrate [5].

The goal of this work is to determine the frequency dependence of losses in 3 different types of filamentary tapes with multiply connected filaments, prepared from YBCO coated conductors. We also compare the obtained results with the loss behavior of a non striated tape and a sample prepared on LaAlO_3 substrate with electrically insulated filaments.

2. Loss components in a filamentary YBCO coated conductor

In samples of filamentary YBCO coated conductors the total losses have several components, as described in [8]. For tapes with relatively wide filaments the main loss components are the hysteresis losses, W_{hyst} , and the coupling losses, W_{coupl} . The hysteresis losses per unit length, P [W/m], in a tape consisting of N_f isolated filament, can be calculated using the formula of Brandt and Indenbom [9], if we neglect the interaction between the filaments:

$$P = 2 f w_f I_{f,c} B_0 [2B_c / B_0 \ln \cosh(B_0/B_c) - \tanh(B_0/B_c)] N_f, \quad (1)$$

where f is the frequency, w_f is the half filament width, $I_{f,c}$ is the critical current in the filament [A/m]. $I_{f,c}$ is supposed to be constant, independent on the local flux density and on the local electric field. The consequence of this assumption is the independence of the per cycle hysteresis loss on the frequency. Herrmann et al.[10] measured the frequency independent hysteresis losses in 0.1 mm wide YBCO strips. However, numerous measurements of $E(I)$ curves in YBCO samples showed that the slope of these curves can be described by the equation $I = I_0(E/E_0)^n$, where n can have values about 30 [11]. The reduction of the filament width below $\sim 100 \mu\text{m}$ causes the reduction of $J_{f,c}$ and n [12]. The effect of the sample length is analysed in [13].

1. Experimental

Sample W/1 has 7 filaments 0.5 mm wide on LaAlO_3 substrate, the width and length of the substrate is 4.8 mm and 40 mm. The striation was made by photolithography and wet etching. The following samples were prepared from coated conductor produced by IBAD method on approximately 100 μm thick, 10 mm wide buffered Hastelloy substrate with YBCO layer subsequently covered by $\sim 3 \mu\text{m}$ thick Ag layer. Laser micromachining was used to striate the samples. The samples are 100 mm long and were cut from 2 longer pieces of coated conductor. The samples B/0, B/1 and B/2 were cut from a tape with the nominal critical current before striation $I_c = 160 \text{ A}$. The samples B/3 and B/4 were cut from a tape with I_c in the range from 120 A to 140 A. The sample B/0 is non striated and B/1 is fully striated with 20 filaments (without superconducting bridges). Samples B/2, B/3 and B/4 are also divided into 20 filaments (approximately 0.5 mm wide each) that are interconnected by superconducting bridges, as shown in Fig.1

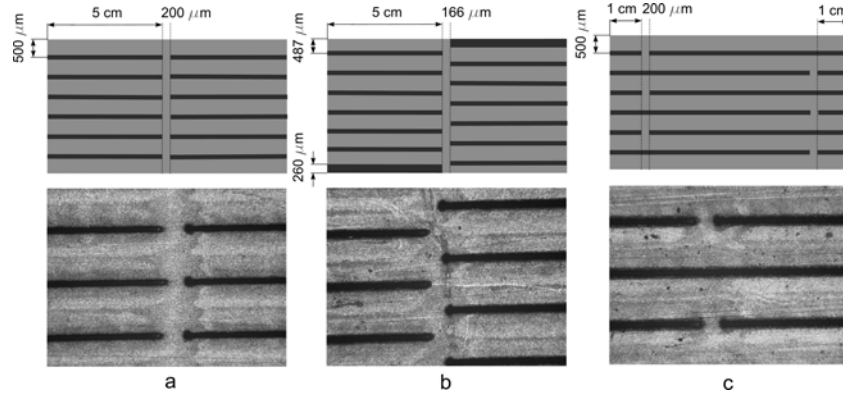


Fig.1: (a) – the sketch and microphotograph of sample B/2, (b) - sample B/3, and (c) - sample B/4.

The losses were measured in a copper dipole coil with the working space with diameter of 40 mm and the field/current constant of 0.97 mT/A at 77 K. At low frequencies (below 0.5 Hz) the losses were measured using pick-up coils and an analog integrator. Above 15 Hz we measured the time dependence of the pick-up coil difference voltage and the losses were determined using the first harmonics obtained by Fourier analysis of the signal.

4. Results and discussion

Fig. 2 shows the measured dependence of the loss per cycle in samples W/1 and W/2. They are pure hysteresis losses. The increase of A_1 per the change of f by the factor of 10 is $\sim 14\%$ and $\sim 15\%$ for W/1 and W/2, respectively.

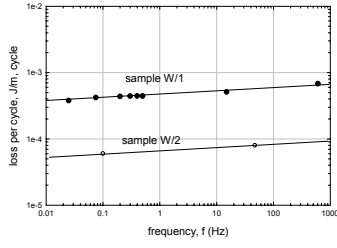


Fig. 2: Loss per cycle A_1 vs. frequency
For samples W/1 and W/2 at $B_m = 54$ mT

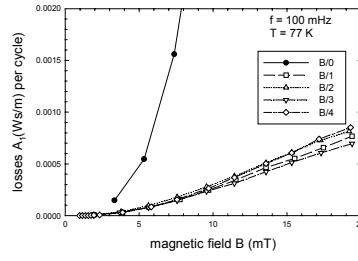


Fig. 3 The hysteresis losses of samples B/0, B/1, B/2, B/3 and B/4 measured at low frequency (100 mHz) and 77 K

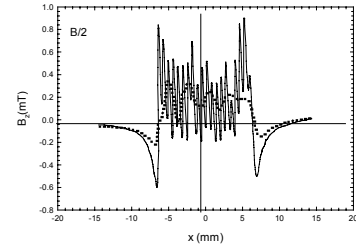


Fig. 4: Magnetic field in the vicinity of sample B/2 carrying magnetization currents

In Fig. 3 we plotted the loss per cycle, A_1 , measured at frequency 100 mHz, when coupling loss is negligible. As expected, the largest loss has sample B/0, the difference of losses in the filamentary samples is relatively small. The smallest hysteresis loss at 20 mT ($\sim 7.2 \times 10^{-4}$ J/m) has sample B/3, losses in sample B/4 are larger by about 25% than those of B/3 ($\sim 9 \times 10^{-4}$ J/m).

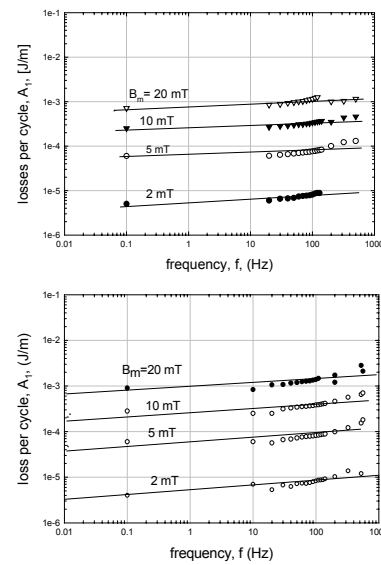
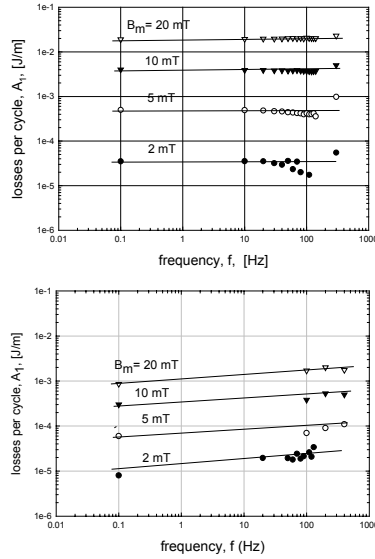


Fig. 5. The dependence of losses per cycle on the frequency of the magnetic field at various field amplitudes: a- sample B/0, b – sample B/2, c- sample B/3, d – sample B/4

We mapped the magnetic field in the vicinity of all samples carrying magnetization currents. The measurements showed that the filament separation in some parts of samples B/2 and B/4 is not perfect, so that the effective sample width is a multiple of the filament width 0.5 mm (see Fig. 4).

In Fig. 5 a, b, c and d we show the losses per cycle of samples B/0, B/2, B/3 and B/4, as a function of the frequency changing from 0.1 Hz to 608 Hz. The largest loss increase has sample B/2 followed by B/4 and B/3. Sample B/0 showed very small increase of losses with increasing frequency ($\sim 5\%$ only).

The hysteresis losses, A , are proportional to the critical current, I_c , which increases with increasing frequency, f , as it is controlled by the electric field $E \sim f$. According to the experiments with W/1 and W/2, the hysteresis losses in samples B/2, B/3 and B/4 at 500 Hz were determined by multiplying the losses determined at 0.5 Hz by the factor $3 \times 12\% = 1.36$ (the value 14 % per the decade of f measured at 54 mT was reduced due to smaller $B_m = 20$ mT to 12 %). The coupling losses at 500 Hz, coupl , were determined by subtracting the hysteresis losses determined

at 500 Hz from the measured total losses. The transverse resistivity ρ_{tr} was calculated using the expression for the coupling losses per unit volume

$$W_{\text{coupl}} = (1/4\rho_{tr})(f B_m 2 L)^2 \quad (2)$$

where L is the sample length and f is frequency. The values of ρ_{tr} obtained for samples B/2, B/3 and B/4 are 2.5×10^{-6} , 1.05×10^{-5} , $3.17 \times 10^{-6} \Omega\text{m}$, respectively. As seen, the values of ρ_{tr} for B/2 and B/4 are close to the resistivity of the substrate ($\sim 1.3 \times 10^{-6} \Omega\text{m}$).

5. Conclusions

The per cycle losses measured in the filamentary YBCO samples with filaments 0.1 mm and 0.5 mm wide at frequencies from ~ 0.1 Hz up to ~ 500 Hz were not frequency independent. They increased with increasing frequency by 10 to 15 % per decade of the frequency. The total loss in our samples of filamentary YBCO coated conductors on Hastelloy substrate is affected by finite inter-filament resistance. This translates into measurable frequency dependence of per cycle loss. Substantial coupling losses were found in all filamentary samples prepared from YBCO coated conductors.

6. Acknowledgements

The financial support from AFOSR, grant number FA8655-03-1-3082 is gratefully acknowledged.

We also acknowledge the support of the Center of Excellence CENG, Slovak Academy of Sciences.

M.P. thanks the Alexander von Humboldt Foundation for the support of the work.

References

- [1] P. N. Barnes, G. L. Rhoads, J. C. Tolliver, M. D. Sumption, K. W. Schmaeman, IEEE Trans. Mag. 41, 268 (2005)
- [2] W. J. Carr, C. E. Oberly, IEEE Trans. Appl. Supercond. **9**, 1475 (1999)
- [3] C. B. Cobb, P. N. Barnes, T. J. Haugan, J. Tolliver, E. Lee, M. Sumption, E. Collings, and C. E. Oberly, Physica C, **382**, 52 (2002).
- [4] M. Polak, L. Krempasky, S. Chromik, D. Wehler, and B. Moenter, Physica C **372-376** (2002) 1830-1834.
- [5] K. E. Hix, M. C. Rendina, J. L. Blackshire, G. A. Levin, cond-mat/0406311
- [6] G. A. Levin, P. N. Barnes, IEEE Trans. on Appl. Superc. 15 (2005) 2158
- [7] N. Amemyia, S. Kasai, K. Yoda, Z. Jiang, G. A. Levin, P. N. Barnes, C. E. Oberly, Supercond. Sci. Technol. 17 (2004) 1464-1471
- [8] Ch. E. Oberly, L. Long, G. L. Rhoads, W. J. Carr Jr., Cryogenics 41 (2001) 117-124
- [9] E. H. Brandt, M. Indenbom, Phys. Rev. B 48 (1993) 12893
- [10] J. Hermann, K.-H. Muller, N. Savvides, S. Gnanarajan, A. Thorley, A. Katsaros, Physica C 341-348 (2000) 2493-2494
- [11] U. Scoop, M. W. Rupich, C. Thieme, D. T. Verebelyi, W. Zhang, X. Li, T. Kodenkandath, N. Nguyen, E. Siegal, L. Civale, T. Holesinger, B. Maiorov, A. Goyal, M. Paranthaman, IEEE Trans. On Appl. Superc. 15 (2005) 2611
- [12] S.I. Kim, D. M. Feldmann, D. C. Larbalestier, D. T. Verebelyi, W. Zhang, C. Thieme, AFOSR HTS Coated Conductor Review, St. Petersburg, FL, January 19-21, 2004
- [13] S. Takacs, F. Gomory, Inst. Phys. Conf. Ser. No. 167 2000 IOP Publishing Ltd., 611-614

APPENDIX B

The determination of current distribution using Hall probe mapping of magnetic field at the vicinity of YBCO tape.

Currents in superconducting tape YBCO generate self magnetic field superposed onto external magnetic field. Appropriate measurement technique allowed to distinguish both and to use the self field data. The measured magnetic fields produced by magnetization currents or transport current can be used to determine the current distribution of these currents across the tape (inverse problem).

The inverse problem was solved in two ways:

- generating inverse matrix relating the mesh of the currents and the mesh of the measured field data, applying Tichonov regularization (details in [Ušák, P.: *The measurements of current distribution in superconducting tape. Comparison of destructive and non-destructive methods*, Physica C **384** \(2003\) 93-101](#)). The number of elements of the vector of current distribution was up to 85.
- minimizing Euclidean norm of vector residui by variation of elements of vector of current distribution as free parameters. The method was more time consuming and more sensitive to measurement errors than the first one. Typical number of elements of current distribution vector was up to 25.

Both methods were tested on numerical models, individually and with respect to each other. Coincidence of results was satisfactory and sometimes even surprisingly good.

The Hall probe magnetometry and the inverse problem solution were applied to two types of YBCO tape:

Both inductive and transport currents were reconstructed from magnetic measurements on samples THEVA and AFOSR P3 ([6.Levin](#)).

Sample THEVA was „homogeneous“ non-striated tape and sample AFOSR P3 was striated (filaments were made by laser) on the most of the tape, except short parts at ends.

Results for the tape THEVA.

In Figure 1a we show the measured magnetic field B_z (perpendicular to the tape plane) induced by external field (decrease from 60 mT to zero level, resp. level 36.5 mT). The current distribution of magnetization currents (in A/m) is shown in Fig. 1b. Zero field data are more concave. Presence of the field $B=36.5$ mT suppressed to some degree the concave character of zero field distribution influenced probably by self field effect (suppressed at the field 36.5 mT)

The tape is not ideally homogeneous. The right part (especially for non zero field current distribution) is more homogeneous than the left part.

Maximum critical current in A/m deduced from inductive measurements (Fig.1b) agrees well with the transport critical currents measurements (Fig.2) and approaches 250A/cm at zero external field.

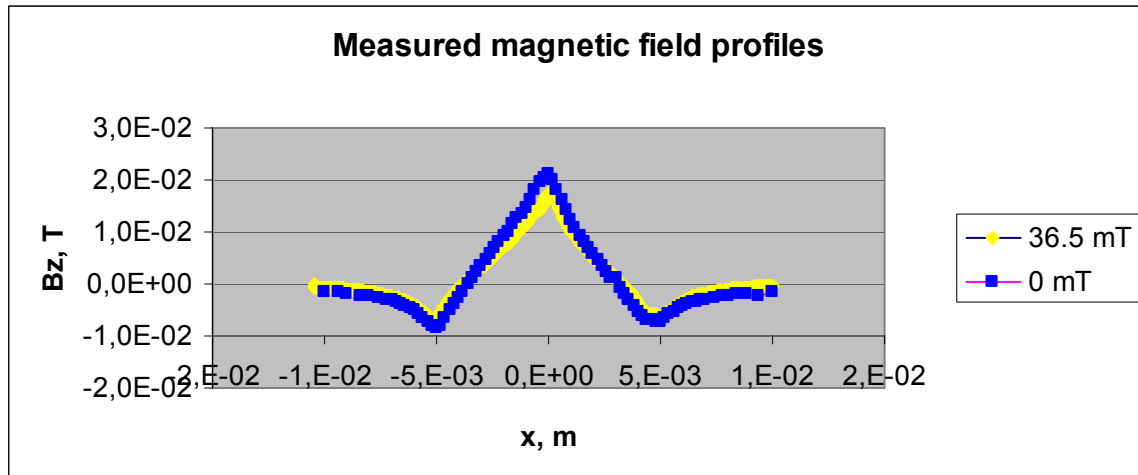


Fig. 1a Measured profiles of magnetic field B_z produced by magnetization currents at different external field.

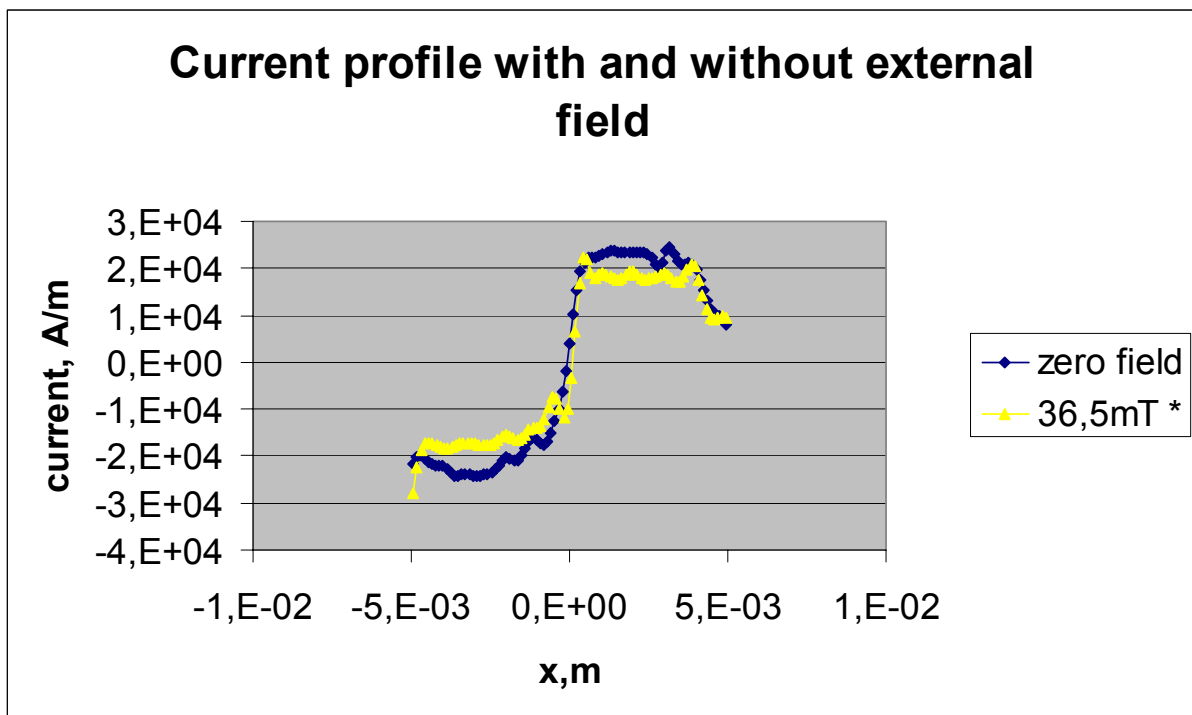


Fig.1b The calculated distribution of magnetization currents, sample THEVA

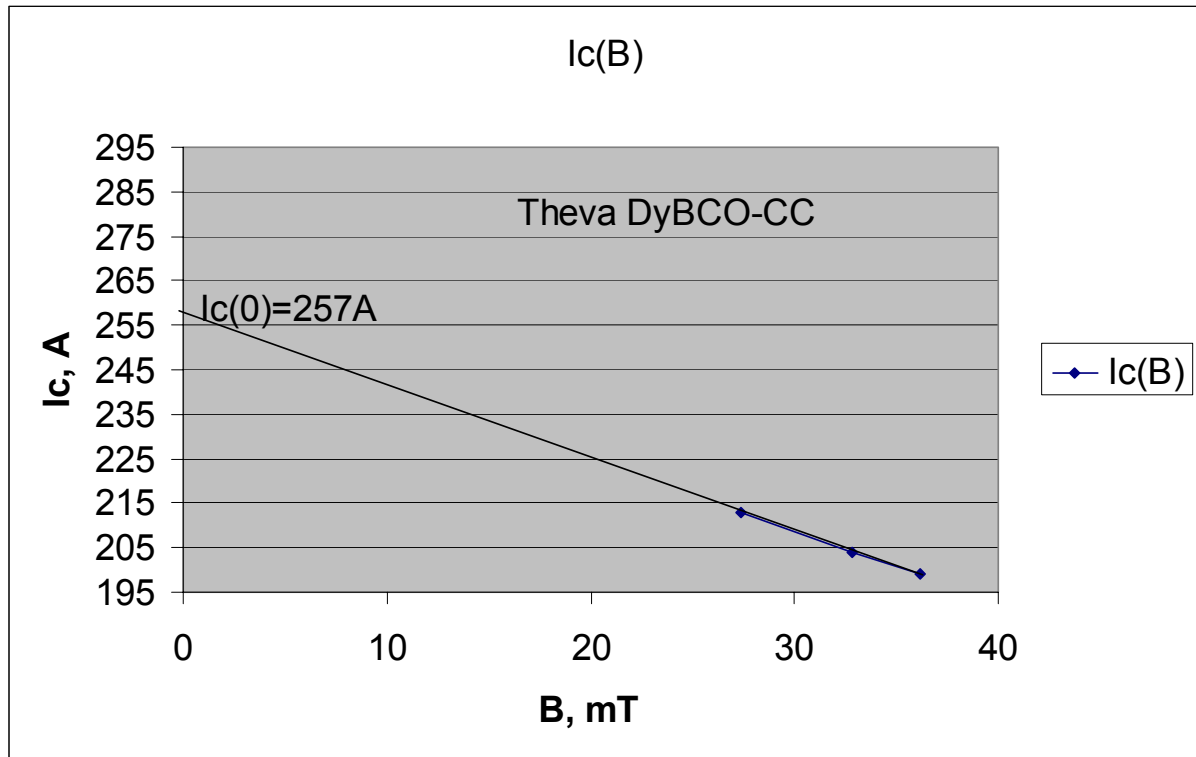


Fig.2 $I_c(B)$ dependence for sample THEVA extrapolated to $B=0T$

The measurements of magnetic field due to the transport current for the tape THEVA were made in zero external field during gradual increase of the current from zero to maximum subcritical level (150A). The results of $B_z = f(I)$ are shown in Fig. 3a and the calculated distribution of current is in Fig. 3b.

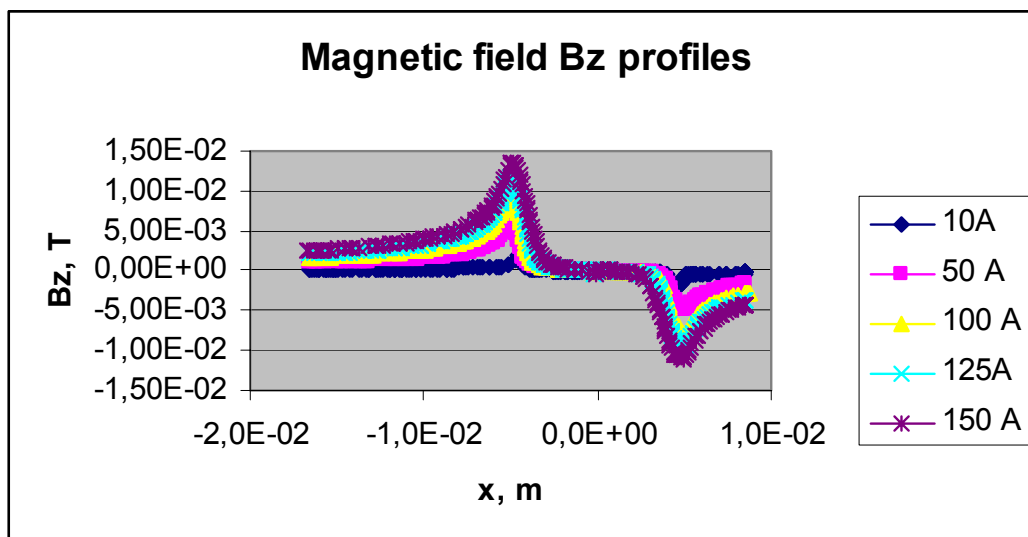


Fig. 3a

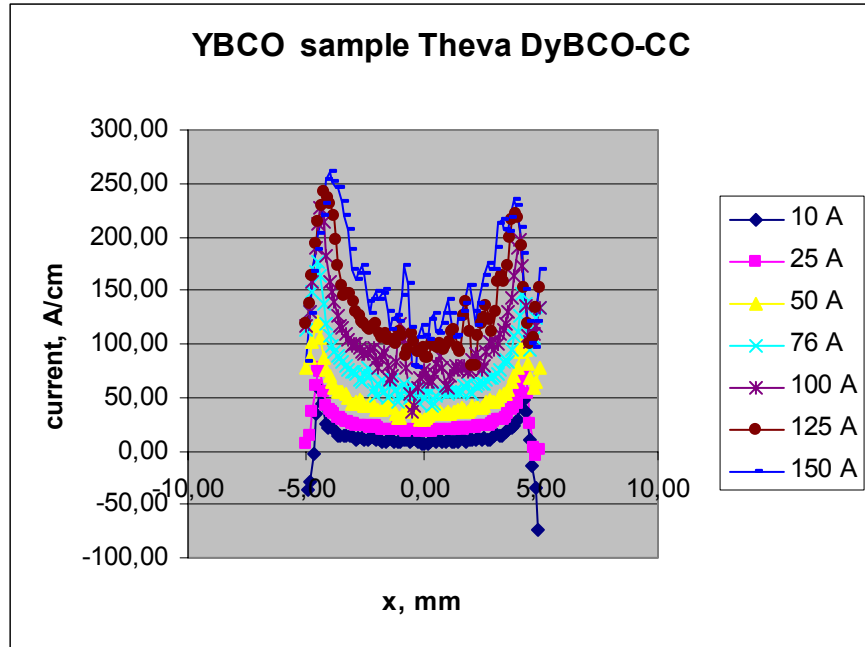


Fig. 3b The calculated distribution of transport current in sample THEVA

Magnetization currents in the tape AFOSR P3

The tape AFOSR P3 was 12 mm wide and 100 mm long. On 15 mm of both sides the YBCO was intact but at central part (70 mm long) there was filamentary zone of 24 filaments 0.5mm wide each. Before striation the critical current of the tape was 160 A (133A/cm). In Fig.4a we show the measured magnetic field B_z over the tape for different values of B increasing from 0 mT up to 63.7 mT. Figure 4b show that zero field full critical current is 120A (data deduced from mapping gradually changed external magnetic field from 0mT to 63.7mT).

Distribution of induced currents is rather complex, with quasi persisting local smaller current loops involving island of filaments on dominant background of filamentary zone. The left part of the tape is more degraded than right one (see Figure 5d with current distributions in zero field, induced during “down” track (used as reference in figures) and “up” track from negative field).

Maximum currents are on right side. However the trend in current distribution is concave on the right side. It is decreasing to edge.

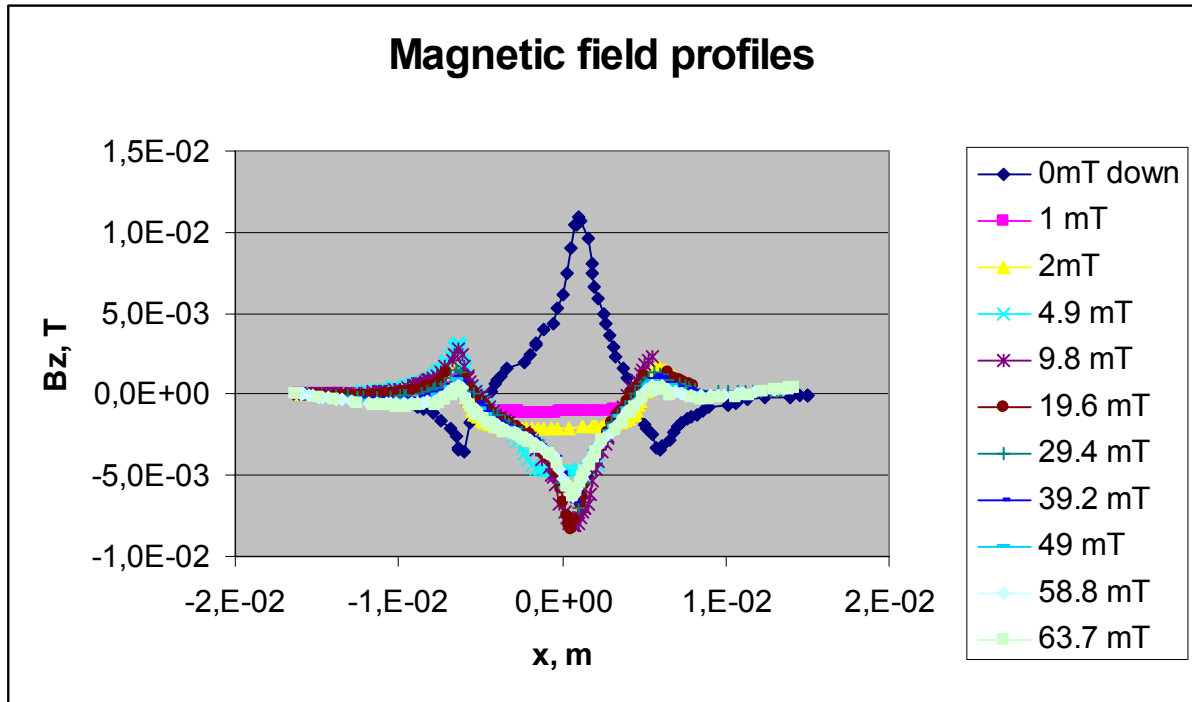


Fig. 4a Measured during gradual field increase and after its decrease to zero level.

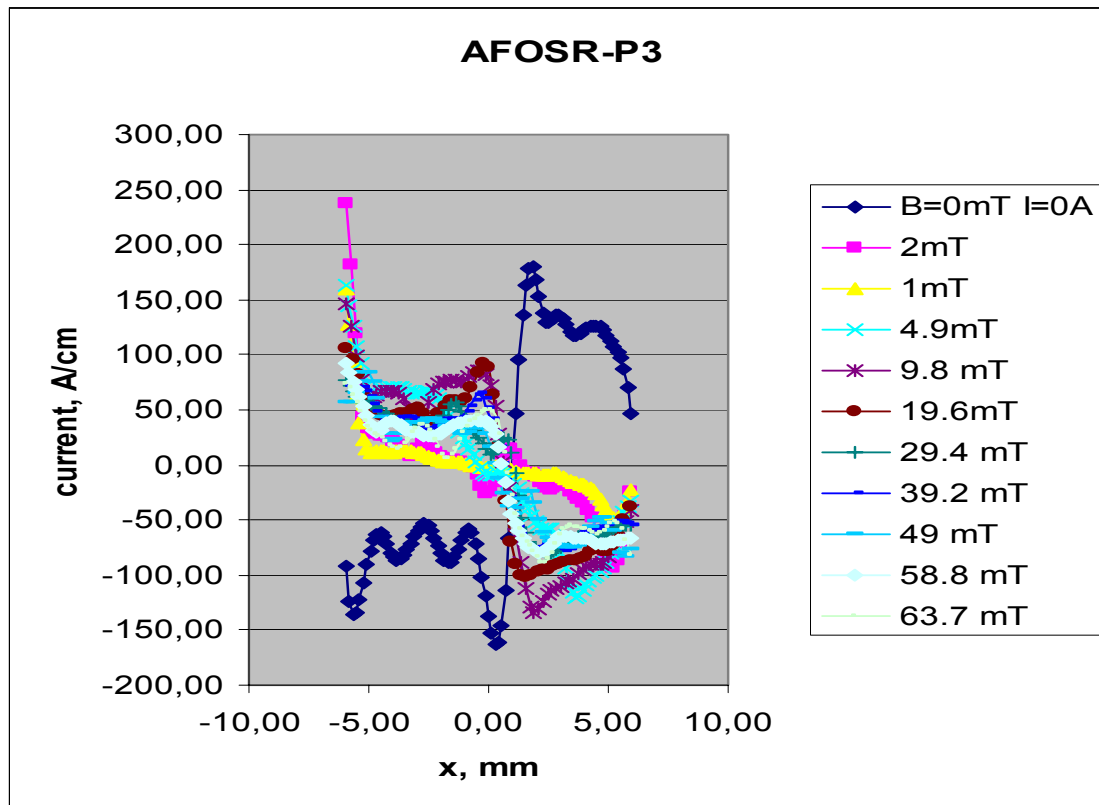


Fig. 4b The calculated distribution of magnetization currents during gradual field increase. The final profile after decrease of external magnetic field to zero level is added.

Conclusion.

The Hall probe mapping/inverse method proved to be useful tool for current distribution measurements in superconducting tapes, including YBCO. It is based on first principles and is direct in nature. It is challenging to check predictions of known theories.

We proved that

- ❖ we can reconstruct current distribution across the tape width from magnetic field mapping by Hall probe magnetometry
- ❖ comparison of full transport current in tape calculated from magnetic field data with experimentally measured transport current gives difference of several percent, most frequently fraction of 1%
- ❖ we can localize damage on the tape and its influence on local current distribution

APPENDIX C

The paper was presented at the International conference on Magnet Technology, Genova, Italy, September 2005, paper TUA 01 PO 05.

It will be published in IEEE Transactions on Magnetics.

Properties of a YBCO pancake coil operating with AC current at frequencies up to 1000 Hz

Milan Polak, Eduard Demencik, Lubomil Jansak, Elo Usak, Pavol Mozola, Cees L. H. Thieme, D. Aized, George A. Levin, Paul N. Barnes

Abstract— A small pancake coil was wound using 1.2 m long, 10 mm wide YBCO coated superconductor tape with impregnation by epoxy resin. The coil was tested in several regimes. In the DC regime, we measured the I-V curve, the hysteresis of the magnetic field-current curve at liquid nitrogen temperature and the radial component of the coil field at the coil edges. The AC losses were measured in the frequency range from 60 Hz to 1000 Hz. The coil was immersed in liquid nitrogen at atmospheric pressure and coil heating due to AC losses was also monitored. The critical currents of a short sample at 77 K were measured and compared with those of the coil. The measured AC losses in the YBCO coil are compared with those of a similar coil wound with copper tape. At 60 Hz, the losses of the YBCO coil were nearly two orders of magnitude lower than those in the Cu coil. With increasing frequency, this difference becomes smaller, but the YBCO coil still exhibited lower losses at 1000 Hz.

Index Terms—Losses, Magnetic fields, Superconducting Magnets

I. INTRODUCTION

The application of YBCO coated conductors in AC devices is often considered, however, the main focus of industry is currently on the improvement of the DC conductor properties such as critical currents. These conductors have the shape of a flat tape several millimeters wide (typically 4 or 10) with thicknesses of the order of 0.1 mm [1]. Typically, a stack of pancake type coils is preferred to make the application windings when using wide tapes. For coils made with Bi-2223/Ag tapes it was shown that the magnetic anisotropy strongly affects the distribution of the current density inside

the tapes [2]. The critical current of the coil is also limited by the largest magnetic field component perpendicular to the tape plane [3]. Since the tape in the pancakes located at the ends of the coil is exposed to an inhomogeneous magnetic field, it is not a straightforward procedure to determine the critical current distribution [4,5]. Similar problems will also appear in coils wound with YBCO coated conductors.

When conductor is placed in an AC environment, the direction of the magnetic field with respect to the wide face of the tape plays an additional important role. According to Brandt and Indenbom [6], the hysteresis loss in YBCO with a transversely applied magnetic field is directly proportional to the tape width [7-9]. Amemiya et al. have shown that in the case of an arbitrary orientation of the magnetic field AC loss are proportional to the transverse component of the field [10]. As such, it is important to have information on the AC behavior of coils made of standard, non-striated YBCO coated conductor. It is of particular interest to obtain ac loss data of a coil at a wide range of frequencies for a better understanding of the ac characteristics of the HTS winding [11]. In this work, we compare the AC behavior of a pancake coil wound with a YBCO coated conductor with that of a similar coil wound of copper tape. Both coils were cooled by liquid nitrogen.

II. EXPERIMENTAL

A. Description of YBCO coil and Cu coil

The YBCO coil was made using a 1.2 m length of copper-stabilized YBCO coated conductor. It was co-wound with wet, epoxy-saturated fiberglass cloth on a G10 coil form, and had an inner and outer diameter of 25.8 mm and 33.8 mm, respectively, after completion. The total number of turns in the winding was 13. Figure 1 is a photograph of the coil.

The conductor was made using a RABiTs architecture: Ni-5 at% W substrate with a sputtered Y_2O_3 seed layer, a YSZ barrier layer, and a CeO_2 cap layer [12]-[13]. The substrate had a Curie temperature of $\sim 60^\circ C$ and is ferromagnetic at 77 K [14], which may contribute to the coil's inductance. The 0.8 μm YBCO layer was deposited using a TFA-based solution process and subsequently capped with a 3 μm Ag layer to which a 50 μm thick Cu 110 foil was laminated. The copper coil was made using a $\sim 110 \mu m$ thick, 1.26 m long copper tape, 10 mm wide, with a resistivity of $1.8 \times 10^{-7} \Omega cm$ at 77 K.

Manuscript received September 20, 2005. This work was supported by AFOSR, grant number FA8655-03-1-3082. We also acknowledge the partial support of the Center of Excellence CENG, Slovak Academy of Sciences. M.P. thanks the Alexander von Humboldt Foundation for the support.

M. P., E. D., L. J., E. U., are with the Institute of Electrical Engineering, Slovak Academy of Sciences, 841 04 Bratislava, Slovakia. Corresponding author M. P.: phone ++421 2 54773545, fax ++421 2 54775816, email elekpol@savba.sk

C. T., D. A. are with the American Superconductor Corporation, Westborough, MA 01581, USA (e-mail CThieme@amsuper.com)

P. B., G. L. are with the Air Force Research Laboratory, Wright-Patterson Air Force Base, OH 45433, USA (e-mail paul.barnes@wpafb.af.mil).



Fig.1. A photograph of the YBCO coil

The number of turns, the inner and outer coil diameter, and the insulation were the same as those of the YBCO coil. A NORMA Power Analyzer 4000D was used to measure the losses of the coil.

III. RESULTS AND DISCUSSION

The DC critical current of the coil using a slowly increasing transport current was 154 A for which the coil voltage was 12 μ V (see Fig. 2). This corresponds to a mean electric field of 0.1 μ V/cm and to a mean current density in the winding cross-section of 5000 A/cm². Optimization of the engineering current density of the windings was not a consideration. At 154 A, the axial field in the coil center, $B_z(r=0)$, is 80 mT and at the inner turn of the coil, $B_z(r=20 \text{ mm})$, is 145 mT calculated assuming a constant current density in the tape.

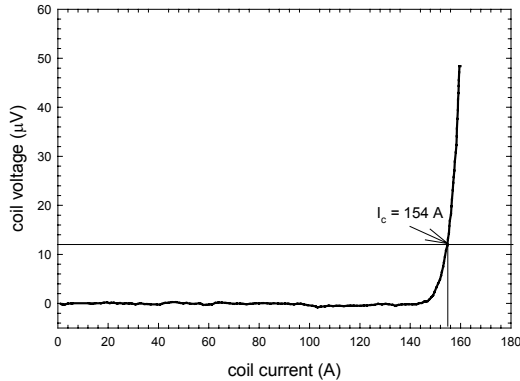


Fig.2. I-V curve of the coil with a DC current, at 77 K.

Using a small active area Hall probe we measured the radial field component, $B_r(r)$, close to the longitudinal edge of the coil ($z = 5.5 \text{ mm}$). In Fig.3 we show the typical set of $B_r(r)$ curves measured at 500 Hz. The radial component of the coil field measured at $z = 5.5 \text{ mm}$ has a maximum, $B_{r,max}$, at $r_m \approx 15 \text{ mm}$ (in the middle of the winding thickness). The measurements were repeated with the coil in the normal state (300 K) carrying a DC current and at 77 K with a DC and then an AC current with frequencies 100 Hz and 1000 Hz. $B_{r,max}$ is plotted vs. coil current in Fig.4. The values of $B_{r,max}$ increase linearly with increasing current at 300 K, but at 77 K they have a hysteretic character and are considerably lower. This behavior further indicates an inhomogeneous current

distribution in the tape.

In Fig. 5, the $B_{r,max} = f(I)$ load line represents the maximal radial magnetic field which is directly proportional to the current (the hysteresis seen in Fig. 4 is not taken into account). The $I_c(B)$ curve represents the critical current of the YBCO conductor when exposed to a uniform external field $B = B_{r,max}$. Since the critical current of the coil (154 A) is considerably higher than the point of intersection of the two curves (90 A), the non-uniformity of the induced magnetic field acting on the tape is clearly an effect that must be considered and that uniform field approximations are not adequate.

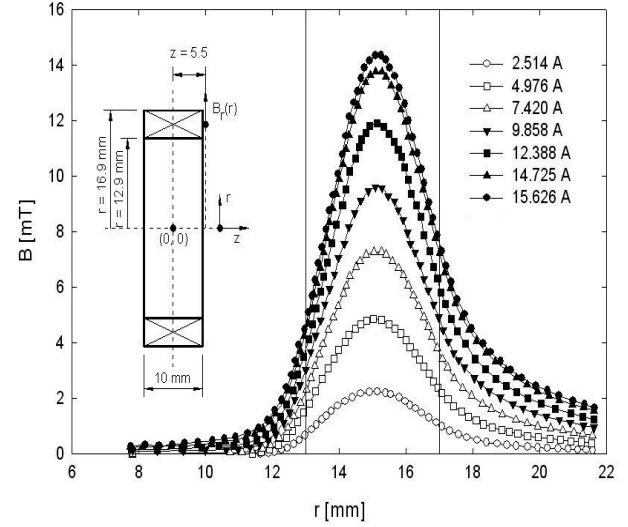


Fig.3 The radial field component, B_r , as a function of the radial position, r , measured at various current (rms) at 500 Hz

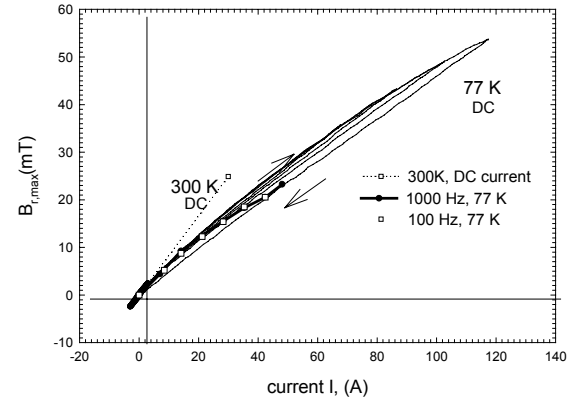


Fig. 4: Maximal values of the radial field component, $B_{r,max}$ (at $r = 15 \text{ mm}$) as the function of current I (peak values) measured at DC current and 77 K (full lines) for 4 different runs $0 \rightarrow I_{max} \rightarrow 0$. The dotted line is the extrapolation of the $B_{r,max}(I)$ curve at 300 K. The curves with AC current were measured at 100 Hz (\bullet) and 1000 Hz (\square).

The uniform field approximation describes the worst scenario (I_c of 90 A), which is almost twice as low as the actual value of the critical current.

An initial improvement to this situation could be made by using B_r for a circular current loop which can be readily expressed in complete elliptic integrals. One would then integrate the expected critical current across the tape due to this field approximation.

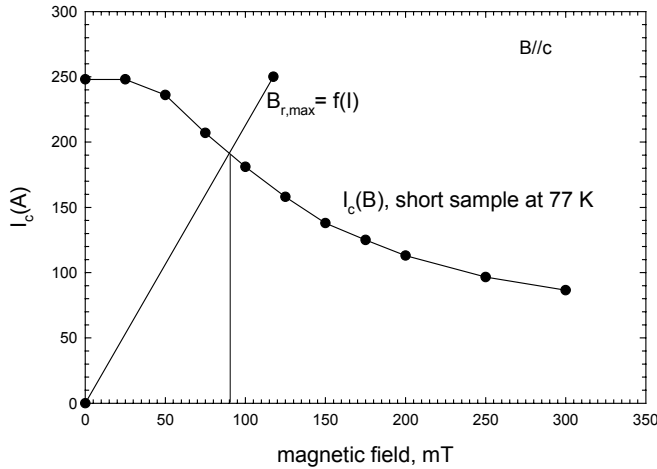


Fig.5. The load line $B_{r,max} = f(I)$ and $I_c(B)$ curve of the YBCO tape used in the coil.

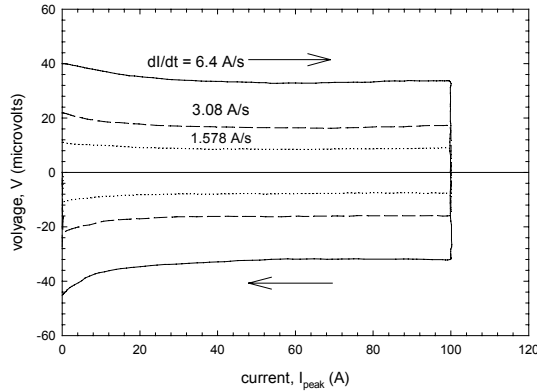


Fig.6 Coil voltage measured vs. current for triangular current waves with $dI/dt = 6.4$ A/s (\bullet), 3.08 A/s (\circ) and 1.578 A/s (\diamond).

The observed behavior of B_r and its non-uniformity demonstrate the need for new procedures to determine ac losses other than simple extrapolation from short sample data.

To determine the coil inductance, L , we recorded the coil voltage, V , while applying triangular transport current waves with the amplitude of 50 A at frequencies of 50 , 100 , and 200 mHz (Fig.6). With $V = L dI/dt$, the shape of the curves shows that L depends on the current at low current values, ranging from ~ 7 μ H at $I = 0$ to ~ 5 μ H with increasing currents. At higher currents, L is current independent which independence tends to shift to higher current levels as dI/dt increases.

Loss measurements for the YBCO coil at frequencies from 60 to 1000 Hz are shown in Fig. 7. We also show the losses of the Cu coil with a DC current and AC currents of 100 and 1000 Hz. There is little difference in losses of the Cu coil between the DC and AC 100 Hz currents. At 1000 Hz, the losses also contain a measurable eddy current contribution. The total losses of both coils increase proportional to I^n , where $n \approx 1.7$ at a frequency of 60 Hz and $n \approx 1.9$ at 1000 Hz. The losses of the copper coil are proportional to I^2 as predicted by theory. However, considerable heating of the Cu coil was

observed at larger currents as deduced from the V-I curve, 8.9 K at $I = 100$ A.

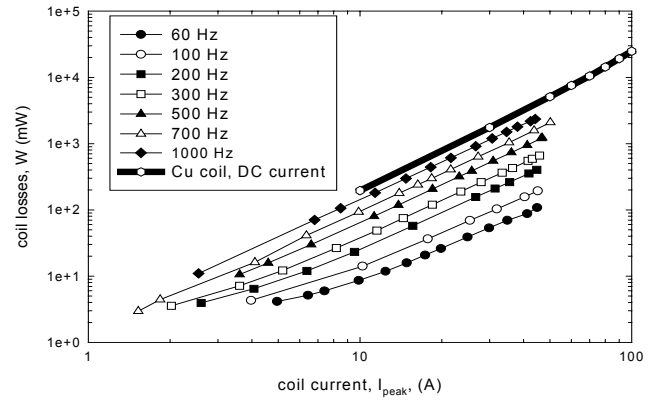


Fig.7 The measured total AC losses of the YBCO and Cu coils as a function of the coil current I_{rms} at various frequencies from 60 Hz (bottom curve) up to 1000 Hz (upper curve). The losses of Cu coil were measured with DC current.

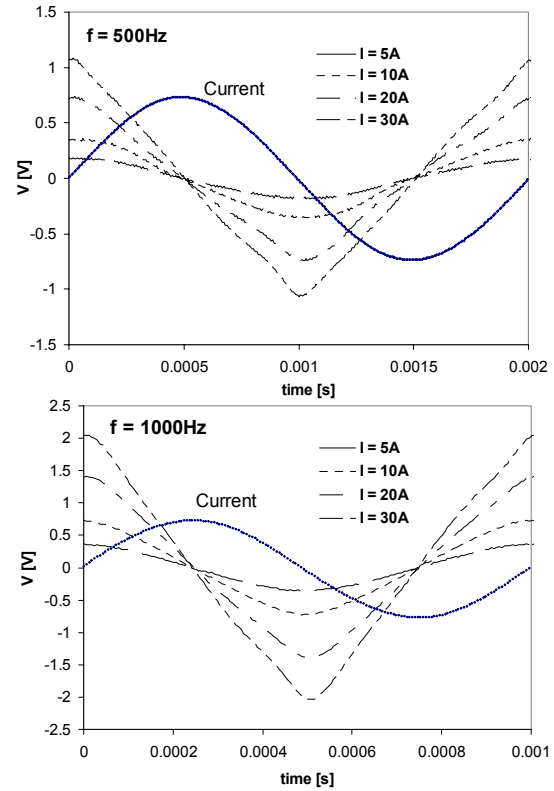


Fig. 8: Coil voltage vs. time t , V , measured at 500 Hz and 1000 Hz at various currents (rms values)

At 60 Hz, the losses in the YBCO coil are nearly 2 orders of magnitude lower than the Cu coil. With increasing frequency, the YBCO coil losses increase and approach the Cu coil losses, but are still smaller at 1000 Hz. The main components of loss in the YBCO are the hysteresis and self-field losses. Of particular interest are the non-sinusoidal voltages measured at higher currents, as seen in Fig. 8. The heating of the YBCO coil was monitored by a copper-constantan thermocouple installed in the winding and was

negligible. At 1000 Hz and with an I_{peak} of 50 A, the temperature increase was below 0.2 K.

- [14] P.N. Barnes, M.D. Sumption, G.L. Rhoads, "Review of High Power Density Superconducting Generators: Present State and Prospects for Incorporating YBCO Windings," Cryogenics, accepted.

IV. CONCLUSIONS

In summary, we measured the AC losses in a small YBCO pancake coil and compared it with a similar coil fabricated in the same fashion using plain copper tape. Due to the magnetization currents, the YBCO coil inductance depends on the coil current. At 60 Hz, the losses of the YBCO coil were nearly two orders of magnitude lower than those in the Cu coil. With increasing frequency, this difference becomes smaller, but the YBCO coil still exhibited lower losses at 1000 Hz. The radial magnetic field component showed that the current distribution in the tape is not uniform. This indicates a need for loss calculation which is suitable for inhomogeneous fields and the need for a more ac-tolerant architecture of YBCO conductor.

REFERENCES

- [1] P.N. Barnes, G.L. Rhoads, J.C. Tolliver, M.D. Sumption, K.W. Schmaeman, "Compact, lightweight superconducting power generator", IEEE Trans. Magn. 41, 2005, pp 268-273
- [2] K. Higashikawa, T. Nakamura, T. Hoshino, "Anisotropic distributions of current density and electric field in Bi-2223/Ag coil with consideration of multifilamentary structure", Physica C 419, 2005, pp.129-140
- [3] J. Pitel, P. Kovac, "Influence of external magnetic fields on critical currents of solenoids wound with anisotropic HTS tapes-theoretical analysis", Supercond. Sci. Technol. 10, 7 (1997)
- [4] J. Kvitkovic, M. Polak, "Current-voltage characteristics of Bi-2223/Ag multifilamentary tapes exposed to inhomogeneous magnetic fields", Physica C 401, 2004, pp. 146-149
- [5] M. W. Rupich, U. Schoop, C. Thieme, D. T. Verebelyi, W. Zhang, X. Li, T. Kodenkandath, N. Nguyen, E. Siegal, L. Civale, T. Holesinger, A. Goyal, and M. Paranthaman, "YBCO coated conductor by an MOD/RABiTS/spl trade/process", IEEE Trans. Appl. Supercond. 15, 2005, pp. 2458-2461
- [6] U. Schoop et al, Annual DOE Peer Review, Washington DC, July 24 2004: <http://www.energetics.com/supercon04.html>
- [7] A. O. Ijoduola, J. R. Thompson, A. Goyal, C. L. H. Thieme, K. Marken, to be published.
- [8] E. H. Brandt, M. Indenbom, "Type II-superconductors strip with current in a perpendicular magnetic field", Phys. Rev. B 48, 1993, p.12 893
- [9] N. Amemiya, T. Nishioka, Z. Jiang, K. Yasuda, "Influence of film width and magnetic field orientation on AC loss in YBCO thin film", Supercond. Sci. Technol. 17, 2004, p. 485
- [10] W. J. Carr, C. E. Oberly, "Filamentary YBCO conductors for AC applications" IEEE Trans. Appl. Supercond. 9, 1999, p. 1475
- [11] C.B. Cobb, P.N. Barnes, T.J. Haugan, J. Tolliver, E. Lee, M. Sumption, E. Collings, and C.E. Oberly, "Hysteresis loss reduction in striated YBCO", Physica C, 382, (2002), p. 52.
- [12] M. D. Sumption, E. W. Collings, P. N. Barnes, "AC loss in striped (filamentary) YBCO coated conductors leading to designs for high frequencies and field sweep amplitudes", Supercond. Sci. Technol. 18, 2005 p. 122
- [13] O. Tsukamoto, "AC losses in a type II superconductor strip with inhomogeneous critical current distribution", Supercond. Sci. Technol. 18, 2005, 596